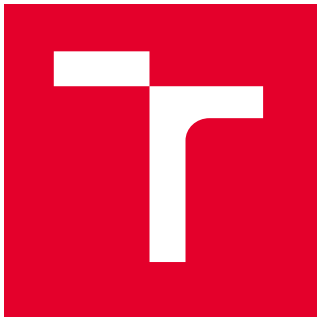

BRNO UNIVERSITY OF TECHNOLOGY

VYSOKÉ UČENÍ TECHNICKÉ V BRNĚ

FACULTY OF MECHANICAL ENGINEERING

FAKULTA STROJNÍHO INŽENÝRSTVÍ

INSTITUTE OF MATHEMATICS

ÚSTAV MATEMATIKY

LUBRICANT GAP SHAPE OPTIMIZATION OF THE HYDRODYNAMIC THRUST BEARING

OPTIMALIZACE TVARU MAZACÍ MEZERY HYDRODYNAMICKÉHO LOŽISKA

MASTER'S THESIS

DIPLOMOVÁ PRÁCE

AUTHOR — **Ikechi Ochulo**

AUTOR PRÁCE

SUPERVISOR — **doc. Ing. Pavel Novotný, Ph.D.**

VEDOUCÍ PRÁCE

BRNO 2021

BRNO UNIVERSITY OF TECHNOLOGY
FACULTY OF MECHANICAL ENGINEERING

Assignment Master's Thesis

Institut:	Institute of Mathematics
Student:	**Ikechi Ochulo**
Degree programm:	Applied Sciences in Engineering
Branch:	Mathematical Engineering
Supervisor:	**doc. Ing. Pavel Novotný, Ph.D.**
Academic year:	2021/22

As provided for by the Act No. 111/98 Coll. on higher education institutions and the BUT Study and Examination

Lubricant Gap Shape Optimization of the Hydrodynamic Thrust Bearing

Brief Description:

Hydrodynamic bearings are designed with maximum mechanical efficiency in mind. Elementary shapes of bearings working surfaces are often assumed when optimizing the bearing performance. The analytical description of elementary shapes thus considerably limits the shape of the work surface. The work deals with the optimization of the working surface of completely general shape. The work assumes the creation of a program or script in a programming language (e.g. Matlab, C ++, Python or Fortran) and application to thrust bearings of turbochargers. It includes a comparison of the integral parameters of the optimal thrust bearing with the existing series–used bearing.

Master's Thesis goals:

Review of suitable optimization methods for solving the problem.
Program for optimizing the bearing working surface of general shape.
Application of the optimization procedure in the design of the working surface of the thrust bearing of a turbocharger.

Recommended bibliography:

LUKE, S. Essentials of metaheuristics. 2. ed., 2013. ISBN 9781300549628.

NGUYEN-SCHÄFER, H. Rotordynamics of Automotive Turbochargers. Second Edition. Ludwigsburg, Germany: Springer, 2015. ISBN 978-3-319-17643-7.

STACHOWIAK, G. W. a A. W. BATCHELOR. Engineering Tribology. 3. vyd. Boston: Elsevier Butterworth-Heinemann, 2005. ISBN 0-7506-7836-4.

Deadline for submission Master's Thesis is given by the Schedule of the Academic year 2021/22

In Brno,

L. S.

.....	.....
prof. RNDr. Josef Šlapal, CSc.	doc. Ing. Jaroslav Katolický, Ph.D.
Director of the Institute	FME dean

Abstract

The objective of this Master's thesis is to find, using genetic algorithm (GA), an optimal profile for lubricating gap of a thrust bearing of a turbocharger. Compared to the analytical profile, the optimal profile is expected to have minimized friction for an equivalent load capacity. Friction minimization is one way to increase the efficiency of the thrust bearing; it reduces the friction losses in the bearing. An initial problem was given: a thrust bearing with Load capacity 1000 N, inner and outer radii of 30mm and 60mm respectively, rotor speed of 45000 rpm and angle of running surface of 0.5^0. Lubricant properties were also provided for the initial problem: oil density of $840kg/m^3$, dynamic viscosity (η) of 0.01 Pa.s With this data, the numerical solution of the Reynolds equation was computed using MATLAB. To obtain more information, the minimum lubricating gap thickness was also computed using MATLAB. With this information, the shape of the analytical profile, and its characteristics were found. The analytical profile was then used a guide to create a general profile. The general profile thus obtained is then optimized using GA. The characteristics of the generated profile is then computed and compared to that of the analytical profile..

keywords

Shape Optimization, Genetic algorithm, Thrust bearing, Lubrication, Turbocharger

Ochulo Ikechi: *Lubricant Gap Shape Optimization of the Hydrodynamic Thrust Bearing*, Brno University of Technology, Faculty of Mechanical Engineering, 2021. 76 pp.
Supervisor: doc.Ing. Pavel Novotný , Ph.D.

I declare that I have worked on this thesis independently under a supervision of doc.Ing. Pavel Novotný, Ph.D. and using the sources listed in the bibliography.

Ikechi Ochulo

To my supervisor , doc. Ing Pavel Novotný, Ph.D. for his guidance and immense patience during the duration of this work.

To friends and family for the support.

To Nkechi.

Ikechi Ochulo

Contents

1 Introduction **12**
- 1.1 The Turbocharger . . . 12
- 1.2 The Bearing . . . 12
  - 1.2.1 Turbocharger Bearing . . . 13
  - 1.2.2 The Hydrodynamic Bearing . . . 13
- 1.3 Problem Definition . . . 14
  - 1.3.1 Description of Working Profile . . . 14
  - 1.3.2 Optimization of Parameters . . . 14
- 1.4 Problem Statement . . . 15
- 1.5 Goal of Thesis . . . 15

2 Literature Review **17**
- 2.1 Introductory Notes on Optimization . . . 17
- 2.2 Optimization Terms . . . 17
- 2.3 Optimization in Thrust Bearings . . . 18
- 2.4 Seminal Works . . . 18
- 2.5 Progress made by seminal works . . . 18
- 2.6 Limitations of the seminal works . . . 19
- 2.7 How does my work fill the gap? . . . 19

3 Materials and Methods **21**
- 3.1 Assumptions of Classical hydrodynamic lubrication theory . . . 21
- 3.2 Reynold's Lubrication Equation . . . 22
  - 3.2.1 Equilibrium of an Element . . . 22
  - 3.2.2 Continuity of Flow in a Column . . . 24
  - 3.2.3 Simplifications to the Reynolds Equation . . . 27
- 3.3 Newton's Method . . . 31
- 3.4 Mathematical description of the Lubricating gap . . . 32
  - 3.4.1 Bearing Pad . . . 32
  - 3.4.2 Bearing Analysis . . . 34
  - 3.4.3 Generalized Gap Profile . . . 41
  - 3.4.4 MultiObjective Optimization . . . 42
- 3.5 Genetic Algorithm . . . 45
  - 3.5.1 Introduction . . . 45
  - 3.5.2 Adaptation of the Genetic Algorithm to our problem . . . 47

4 Results and Discussions **48**
- 4.1 Initial Problem . . . 48
  - 4.1.1 Analytical Results . . . 50
  - 4.1.2 Numerical Results . . . 50
- 4.2 General Gap Profile . . . 53
- 4.3 Scalarization of Objective function . . . 54
- 4.4 GA Results . . . 56
- 4.5 Optimal Gap Profile . . . 56
- 4.6 Discussion . . . 57
  - 4.6.1 Analytical and General Gap Profile Results . . . 57

4.6.2 Analytical and Optimized Profile Results 58

5 Conclusion **59**
5.1 Parameter Choice 59
5.2 Genetic Algorithm: Strengths and Weaknesses 59
5.2.1 Strengths 59
5.2.2 Weaknesses 59
5.2.3 Measures Taken to Mitigate Weaknesses 60
5.3 Working Profile Description 60
5.4 Why is the working profile better? 60
5.5 Application of Study 61
5.6 Future Work 61

6 References **62**

7 APPENDIX **66**

1 Introduction

1.1 The Turbocharger

A turbocharger is a rotor that features a turbine on one side and a compressor on the other side.

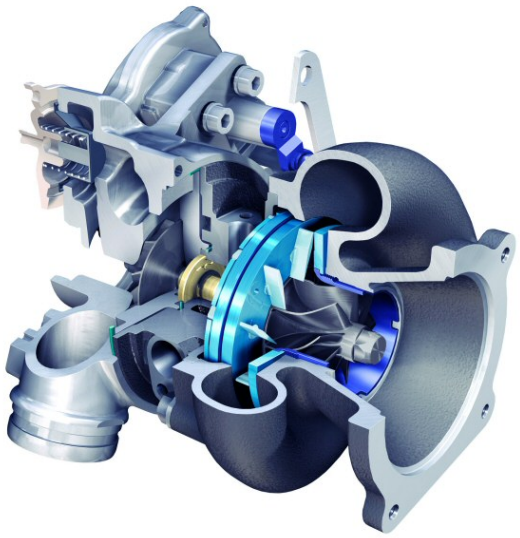

Figure 1: Borg-Warner Turbocharger with Variable Geometry Turbine
[1]

Turbochargers have improved the efficiency of combustion engines while reducing their size and maintaining the power. In recent times, most diesel engines are turbocharged; more gasoline engines are also being equipped with the turbocharger.

In passenger vehicles, the turbocharger scavenges from the exhaust gas flow. The compressor compresses the surrounding air and feeds it to the engine.

1.2 The Bearing

A bearing is a machine part that bears (supports) one or more of the moving parts of a mechanical assembly. Its principal function is to reduce mechanical friction between the moving parts. By reducing friction, it improves the efficiency of running, reduces abrasion and wear due to friction and improves the life of the machinery.

To reduce the effects of friction among the moving parts of mechanical assemblies, the surfaces of these parts are lubricated. It is expected that the lubricating fluid be viscous enough, and maintain this property under high temperature; the fluid should be able to carry the heat generated by these moving parts away from the surfaces, hence cooling these surfaces.

1.2.1 Turbocharger Bearing

The fluid film bearing system of a turbocharger commonly comprises the three regimes of lubrication: boundary, mixed and hydrodynamic.[2]

The mixed and boundary regimes of lubrication do not provide an optimal operating environment for the turbocharger. In these regimes, there is the risk of high wear of the component parts of the turbocharger [3]. To prevent operating in these regimes , the oil film thickness should be larger than the limit oil film thickness of 3 micrometers (3 x 10^{-6} m).

1.2.2 The Hydrodynamic Bearing

When the surfaces of the two moving parts glide over each other with sufficient velocity for a load-carrying lubricating film to be generated and these surfaces are inclined at an angle to each other, hydrodynamic lubrication occurs.

A hydrodynamic bearing supports a shaft in hydrodynamic lubrication. Pressure in the hydrodynamic film is generated due to relative motion of the surfaces separated by the layer of viscous fluid [4].

In our problem, we consider the movement of two parts of a mechanical assembly: the thrust rings and the shaft. The thrust bearing supports the axial motion of the shaft.

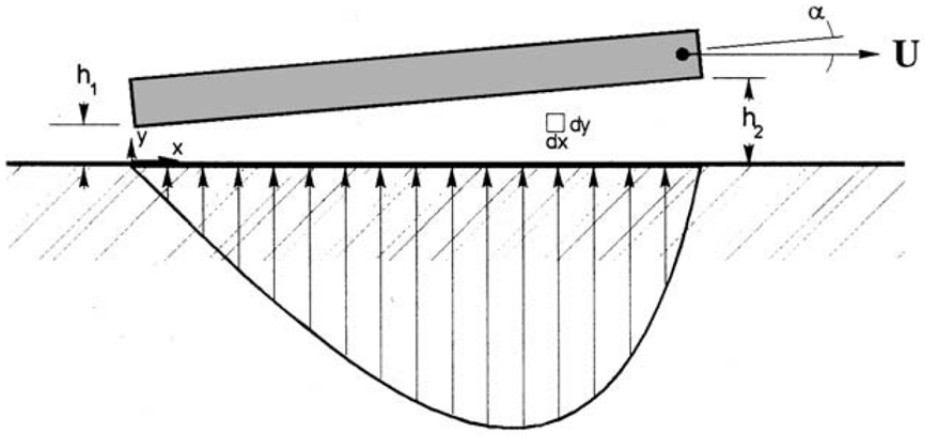

Figure 2: Schematic of Hydrodynamic Bearing
[3]

Schematically, this setup could be represented as an inclined plane-slider carrying a load F, with a horizontal velocity U, relative to a stationary horizontal plane surface. This plane-slider has an angle of inclination α relative to the horizontal plane. Fig.(2)

At full hydrodynamic lubrication, a full separation between the plane-slider and the horizontal plane surface is obtained. The inclined slider forms a converging viscous wedge

of lubricant; the magnitudes of h_1 and h_2 are very small. The clearance is very much enlarged.

The wedge that is formed by the lubricating fluid takes the shape of the clearance between the two components being lubricated. The shape of this clearance is called the lubricating gap [3].

1.3 Problem Definition

It has always been the goal of engineering to improve design to satisfy the human need in the best way possible, within available means.

The classical approach to optimization of the thrust bearing was:

1 Describing the bearing analytically by parameters

2 Optimizing these parameters by any optimization method

In recent times and for this work, the new approach to optimization:

1. Describing the working profile of the bearing a general function

2. Optimizing parameters by any optimization method.

1.3.1 Description of Working Profile

The working profile under consideration is the lubricating gap of the thrust bearing.
The lubrication gap in a hydrodynamic thrust bearing exerts great influence of the on the bearing properties. It has been shown from experiments that a close-to-optimum oil gap profile for assumed load/speed conditions, the results show substantial increase in the minimum oil film thickness and lower temperature in the bearing. This improvement of properties is thought to be because of the optimized oil gap profile in the bearing [5].

1.3.2 Optimization of Parameters

Design optimization is, in layman terms, the procedure of finding and/or selecting the best way to implement a design, within available means.

For this problem, the parameters are the various sizes of the lubricating gap that make up the lubricating gap profile.

The evolutionary algorithm would be used to optimize these parameters. In particular, the lubricating gap profile would be optimized using the Genetic Algorithm.

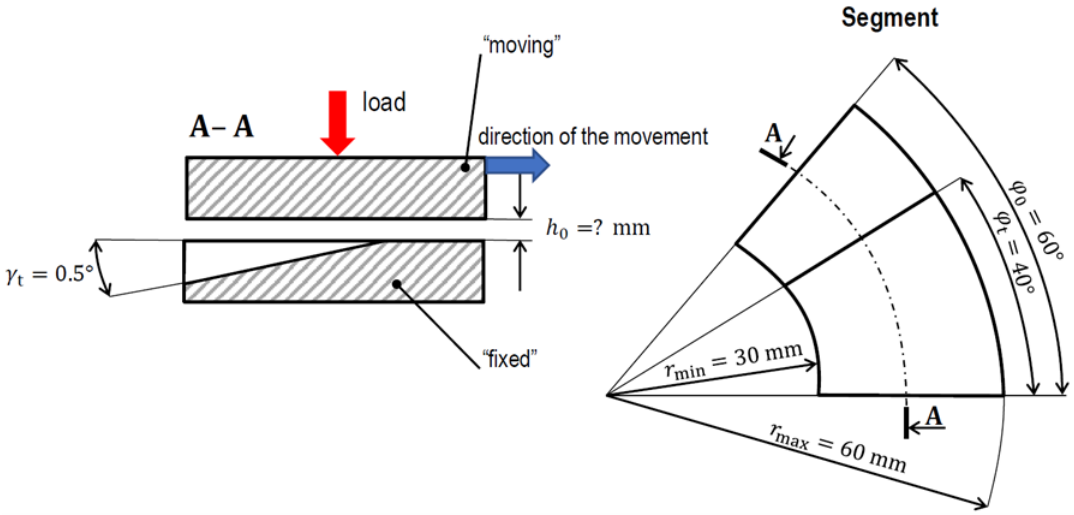

Figure 3: Initial Problem

1.4 Problem Statement

The initial problem Fig.(3) has the following given values:

Load segment $F_{ax} = 1000N$

Rotor speed, n = 45000 rpm

Lubricant dynamic viscosity, $\mu = 0.01$ Pa.s

The criteria under which the problem is to be solved:

i Minimize friction force.

ii Maintain load capacity.

iii Do not increase lubrication flow rate.

iv Do not decrease minimum gap thickness.

For the scope of this work:

i The problem will be considered in two dimensions.

ii Optimization will be done using genetic algorithms.

1.5 Goal of Thesis

The genetic algorithm was implemented to solve this problem.
Genetic algorithms are stochastic methods that can be used to solve approximately in

optimization. It attempts to replicate the dynamics of natural selection and genetics. A randomly selected parent population (elements from the set of admissible shapes) reproduces and mutates to form offspring (new shapes) under the condition that only the fittest survive.

To find an optimal profile for the given problem would involve sorting and testing of all elements of the set of admissible shapes and keeping the most optimal of them.

This algorithm randomly tests all possible solutions: keeping the optimal shapes and discarding the least optimal ones. With the aid of genetic algorithms, we hope to find an optimal general lubrication gap profile that satisfies the constraints of the optimization problem.

2 Literature Review

2.1 Introductory Notes on Optimization

The role of shapes of materials has been assumed for the most of technological advancement. It was generally assumed that smooth surfaces should result in better tribological performance of engineering instruments and equipment. This assumption was extended to the general objects in our surrounding. The thought that fostered this assumption was that to eliminate friction, the surfaces in contact should be smoothened, given a better finish [6].

But this is not true. The cutting of groves (or dimples) in the golf ball made it possible for the club to get a better 'grip' of the ball; this was consistent with the prevailing thought and expectations. What was unexpected was the fact that these groves made the flight of the ball through air (a fluid) better; the ball could move more smoothly, and it also moved farther than the smooth ball. This makes the case for the study of optimization of surfaces and shapes interacting in fluid media. Smoothening the sole of a shoe would reduce friction between the shoe and the ground; but that is not the case when considering objects like the golf ball or bearings.

Apparently, this was already practiced by nature. The microstructures on the skin of the shark helped reduce drag in its movement through water.[7].

2.2 Optimization Terms

Before formulating the optimum design problems for high-speed, journal bearings, the terms and definitions used in optimum design:

- Design variable: the main factor that determines bearing design. Radial clearance, bearing length, bearing radius and viscosity come under the scope of design variables.
- State variable: physical quantities that vary under operating conditions such as the load, rotational speed, eccentricity ratio quantity of lubricant supply, etc.
- Constraint: a condition that must be satisfied in the optimum design. It might include restrictions relatable to film thickness, film temperature or pressure, etc.
- Objective function: the quantity, function, to be minimized or maximized under the constraints. This includes fluid temperature rise, quantity of lubricant supplied, manufacturing cost, etc.
- Optimum design problem: the problem of finding the optimum variables that optimize the objective function under the prescribed constraints [8].

2.3 Optimization in Thrust Bearings

The principal performance indices of a thrust bearing are its load carrying capacity and its friction coefficient. Optimizing thrust bearing performance would mean either the maximization of load carrying capacity or minimizing the friction coefficient.

Maximizing the load capacity of the thrust bearing would lead to larger film thickness for a given load and by implication less bearing wear. Increasing the film thickness would also better the bearing performance in transient or impact loads.

Minimization of the friction coefficient will contribute to reduced power losses. [2]

2.4 Seminal Works

The idea of modification of the shapes (and texture of surfaces) of tribological parts of mechanical devices to improve performance has been hinted in the introduction; it has been evident in nature. However, the application of this knowledge is quite recent.

Lawrence J. Fogel's dissertation, "*On the Organization of Intellect*" was undoubtedly the first such thesis, if not the first major work, in the field of evolutionary computation. [9].

The Genetic Algorithm was invented by John Holland at the University of Michigan in 1975. His book *Adaptation in Natural and Artificial Systems*published by the University of Michigan Press is one of the more famous books in the field.

The idea of using Genetic Algorithms (GA) in Engineering design was first introduced by The Plymouth Engineering Design Center (PEDC) in 1991. The center was established to carry out fundamental research into the application of Genetic Algorithm and adaptative search techniques to engineering design. It has as one of its missions, the making of GA more accessible to practicing engineers across a wide range of disciplines. This goal has since made the center to string along different branches of engineering and has kept its research and works to remain the domain of applicability. The goal has been to make the algorithm accessible in a useful and understandable form to designers engaged in the many branches of engineering. It was envisaged that GA oriented design process can be developed with which the engineer will be able to interact to reduce design time whilst also significantly improving both performance and the economics of the design solution. [10]. They also investigated ways to integrate GA into existing design practices.

2.5 Progress made by seminal works

"*One of the ways to reduce the friction losses in a turbocharger thrust bearing is by application of surface texture features. Recent research has been carried out to investigate the effect of periodic irregularities of various shapes (rectangular, trapezoidal, cylindrical or spherical), imprinted on part of the stator of fixed inclination thrust bearings on bearing performance. The reported numerical and experimental studies, demonstrated po-*

tential for improving bearing performance. As current technology has enabled the accurate manufacturing of such micro-scale patterns, contemporary research on the performance of textured bearings is growing more intense, with the optimization of texture geometry and placement being attempted by several researchers.[2]"

Most of the recorded progress in this field has been in the texture of the surface of the lubricated mechanical parts. Many research groups have deliberated, by theory and experimentation, the effect of various shape contours of textures on tribological performance. They confirmed that different texture shapes affect the tribological performance of the lubricating system.

In their work, Charitopoulos et al [2], experimented the optimization of tapered-land bearing. The geometric parameters used for the optimization of the tapered-land bearing were:

- the extent of the tapered part of the bearing as percentage of the length, and
- the maximum taper depth in microns.

Most of the work in thrust bearing optimization, have considered optimizing the tapered-land bearing. Its fixed geometry has made it attractive for analysis.

2.6 Limitations of the seminal works

Modification of the shape of mechanical equipment and parts has been 'restricted' to aerodynamics. The shape of the body in motion has been necessary in the improvement of the performance of cars, bicycles, airplanes, and other mechanical devices. This has been proven to reduce the drag of the vehicle, reduce the fuel consumption, and improve the general efficiency of the vehicle.

However, this idea of shape modification and optimization has not been exhaustively applied to lubricated parts of these vehicles. This means that the idea of shape optimization has not seen extensive application in the tribology. The limited application of the knowledge of shape optimization to tribology means that a lot more progress can be made in reducing friction, increasing load capacity, and improving the efficiency of mechanical systems.

The consideration of simple profiles presents an easier problem. But, it has limited the scope of what is known of the working conditions of the tilted-pad bearings with variable geometry.

2.7 How does my work fill the gap?

As stated above, the thrust bearing is optimized by increasing the load capacity or minimizing friction coefficient. Minimizing the friction coefficient improves the mechanical efficiency of the setup.

The mechanical efficiency of the turbocharger plays a vital role in determining the general efficiency of the turbocharger. This means that an improvement of the mechanical efficiency of the turbocharger will influence the general efficiency of the turbocharger.

Maximizing the load capacity of the thrust bearing would lead to larger film thickness for a given load. This results in less bearing wear.

Finding the optimal lubrication gap profile for the turbocharger under the given constraints would result in better mechanical effects in the system. It would minimize friction in the system and thus improve the mechanical effects and efficiency of the system. It would also maximize the load capacity of the bearing reducing the rate of wear of the bearing.

3 Materials and Methods

3.1 Assumptions of Classical hydrodynamic lubrication theory

1. The flow is laminar because the Reynolds number, Re, is low.

2. The fluid lubricant is continuous, Newtonian, and incompressible.

3. The fluid adheres to the solid surface at the boundary and there is no fluid slip at the boundary; that is, the velocity of fluid at the solid boundary is equal to that of the solid.

4. The velocity component, n, across the thin film (in the y direction) is negligible in comparison to the other two velocity components, u and w, in the x and z directions as can be seen in Figure**??**.

5. Velocity gradients along the fluid film, in the x and z directions, are small and negligible relative to the velocity gradients across the film because the fluid film is thin, i.e., $du = dy >> du = dx$ and $dw = dy >> dw = dz$..

6. The effect of the curvature in a journal bearing can be ignored. The film thickness, h, is very small in comparison to the radius of curvature, R, so the effect of the curvature on the flow and pressure distribution is relatively small and can be disregarded.

7. The pressure, p, across the film (in the y direction) is constant. In fact, pressure variations in the y direction are very small and their effect is negligible in the equations of motion.

8. The force of gravity on the fluid is negligible in comparison to the viscous forces.

9. Effects of fluid inertia are negligible in comparison to the viscous forces. In fluid dynamics, this assumption is usually justified for low-Reynolds-number flow.

10. The fluid viscosity, η, is constant. This is for simplification of the analysis.

This last assumption can be applied in practice because it has already been verified that reasonably accurate results can be obtained for regular hydrodynamic bearings by considering an equivalent viscosity. [11]

For a proper analysis of the problem, and optimization of the lubrication gap profile of the thrust bearing, the tools of analysis to be used include:

- Reynold's equation
- Newton's Method
- Mathematical description of the lubricating gap

- Genetic algorithm
- MATLAB

3.2 Reynold's Lubrication Equation

The Reynolds lubrication equation is used to compute the flow dynamics and included bearing forces in the oil film bearings. It works with insignificantly small convection terms at low Reynolds number. This is because the oil flows in oil film bearings of automotive turbochargers are usually laminar having Reynolds number ranging from 100 to 200 [3].

3.2.1 Equilibrium of an Element

The equilibrium of an element of fluid is considered. This approach is frequently used in engineering to derive formulae in stress analysis, fluid mechanics, etc.

Consider a small element of fluid from a hydrodynamic film shown in Fig.(4). For simplicity, assume that the forces on the element are acting initially in the ' $\mathbf{x}'$ direction only. Since the element is in equilibrium, forces acting to the left must balance the forces acting to the right, so

$$\mathbf{pdydz} + \left(\tau_{\mathbf{x}} + \frac{\partial \tau_x}{\partial \mathbf{z}}\mathrm{dz}\right)\mathrm{dxdy} = \left(\mathbf{p} + \frac{\partial \mathbf{p}}{\partial \mathbf{x}}\mathbf{dx}\right)\mathbf{dydz} + \tau_{\mathbf{x}}\mathrm{dxdy} \tag{3.1}$$

which after simplifying gives:

$$\frac{\partial \tau_x}{\partial z}dxdydz = \frac{\partial p}{\partial x}dxdydz \tag{3.2}$$

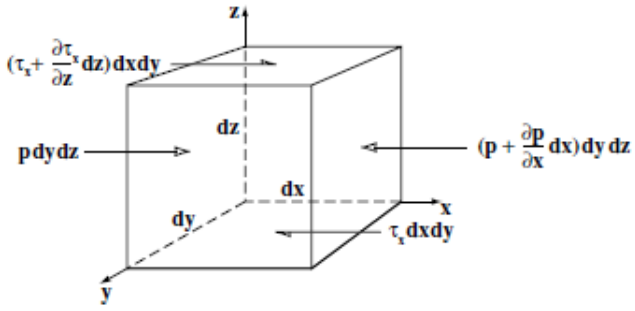

Figure 4: Equilibrium of an element of fluid from a hydrodynamic film

p is the pressure, τ**x** is the shear stress acting in the 'x' direction.

Assuming that d$x$dyd$z \neq 0$ (i.e., non zero volume), both sides of equation (3.2) can be divided by this value and then the equilibrium condition for forces acting in the ' x ' direction is obtained,

$$\frac{\partial \tau_{\mathrm{x}}}{\partial \mathbf{z}} = \frac{\partial \mathrm{p}}{\partial \mathbf{x}} \tag{3.3}$$

A similar operation can be performed for the forces acting in the ' y' (out of the page) direction, yielding the second equilibrium condition,

$$\frac{\partial \tau_y}{\partial \mathbf{z}} = \frac{\partial \mathbf{p}}{\partial \mathbf{y}} \tag{3.4}$$

In the ' z′ direction, since the pressure is constant through the film (Assumption 7), the pressure gradient is equal to zero:

$$\frac{\partial \mathbf{p}}{\partial \mathbf{z}} = \mathbf{0} \tag{3.5}$$

It should be noted that the shear stress in equation (3.3) is acting in the ' x ' direction while in equation (3.4) it is acting in the ' y ' direction, thus the values of the shear stress in these expressions are different.

The formula for dynamic viscosity, calculated from the shear stress τ', can be expressed in terms of dynamic viscosity and shear rates:

$$\tau_{\mathrm{x}} = \eta \frac{\mathbf{u}}{\mathbf{h}} = \eta \frac{\partial \mathbf{u}}{\partial \mathbf{z}} \tag{3.6}$$

where: τ_x is the shear stress acting in the ' x ' direction [Pa].

Since ' u′ is the velocity along the $'\boldsymbol{x}'$ axis, the shear stress ' τ' is also acting along this direction. Along the ' y' (out of the page) direction, however, the velocity is different and consequently the shear stress is different:

$$\tau_y = \eta \frac{v}{h} = \eta \frac{\partial \mathbf{v}}{\partial \mathbf{z}} \tag{3.7}$$

where: τ_y is the shear stress acting in the $'$y$'$ direction [Pa]; $\mathbf{y}$ is the sliding velocity in the ' $\mathbf{y}$ ' direction [m/s]. Substituting 3.6 into 3.3 and 3.7 into 3.4, the equilibrium conditions for the forces acting in the ' x' and ' y ' directions are obtained:

$$\frac{\partial \mathbf{p}}{\partial \mathbf{x}} = \frac{\partial}{\partial \mathbf{z}} \left(\eta \frac{\partial \mathbf{u}}{\partial \mathbf{z}} \right) \tag{3.8}$$

$$\frac{\partial \mathbf{p}}{\partial \mathbf{y}} = \frac{\partial}{\partial \mathbf{z}} \left(\eta \frac{\partial \mathbf{v}}{\partial \mathbf{z}} \right) \tag{3.9}$$

Equations (3.8) and (3.9) can now be integrated. Since the viscosity of the fluid is constant throughout the film (Assumption 10) and it is not a function of ' z' (i.e., $\eta \neq f(z)$), the process of integration is simple. For example, rewriting (3.8),

$$\frac{\partial \mathbf{p}}{\partial \mathbf{x}} \mathbf{dz} = \eta \frac{\partial^2 \mathbf{u}}{\partial \boldsymbol{z}^2} \tag{3.10}$$

and integrating gives:

$$\frac{\partial \mathbf{p}}{\partial \mathbf{x}} \mathbf{z} + \mathbf{C}_1 = \eta \frac{\partial \mathbf{u}}{\partial \mathbf{z}} \tag{3.11}$$

Separating variables again,

$$\left(\frac{\partial p}{\partial x}z + C_1\right) dz = \eta du \tag{3.12}$$

and integrating again yields:

$$\frac{\partial \mathbf{p}}{\partial \mathbf{x}}\frac{\mathbf{z}^2}{2} + \mathbf{C}_1\mathbf{z} + \mathbf{C}_2 = \eta\mathbf{u} \tag{3.13}$$

Since there is no slip or velocity discontinuity between liquid and solid at the boundaries of the wedge, the boundary conditions are:

$$\begin{aligned} \mathbf{u} &= \mathbf{U}_2 \quad \text{at} \quad \mathbf{z} = \mathbf{0} \\ \mathbf{u} &= \mathbf{U}_1 \quad \text{at} \quad \mathbf{z} = \mathbf{h} \end{aligned} \tag{3.14}$$

In the general case, there are two velocities corresponding to each of the surfaces ' $\mathbf{U}_1$ ' and $'\mathbf{U}_2'$. By substituting these boundary conditions into (3.13) the constants ' C_1' and ' C_2' are calculated:

$$\begin{aligned} \mathbf{C}_1 &= (\mathbf{U}_1 - \mathbf{U}_2)\frac{\eta_1}{\mathbf{h}} - \frac{\partial \mathbf{p}}{\partial \mathbf{x}}\frac{\mathbf{h}}{2} \\ \mathbf{C}_2 &= \eta\mathbf{U}_2 \end{aligned} \tag{3.15}$$

Substituting these into (which equation) yields:

$$\frac{\partial \mathbf{p}}{\partial \mathbf{x}}\frac{\mathbf{z}^2}{2} + (\mathbf{U}_1 - \mathbf{U}_2)\frac{\eta\mathbf{z}}{\mathbf{h}} - \frac{\partial \mathbf{p}}{\partial \mathbf{x}}\frac{\mathbf{hz}}{2} + \eta\mathbf{U}_2 = \eta\mathbf{u} \tag{3.16}$$

Dividing and simplifying gives the expression for velocity in the ' x ' direction:

$$\mathbf{u} = \left(\frac{\mathbf{z}^2 - \mathbf{zh}}{\mathbf{2}\eta}\right)\frac{\partial \mathrm{p}}{\partial \mathbf{x}} + (\mathbf{U}_1 - \mathbf{U}_2)\frac{\mathbf{z}}{\mathbf{h}} + \mathbf{U}_2 \tag{3.17}$$

In a similar manner a formula for velocity in the $'\mathbf{y}'$ direction is obtained.

$$\mathbf{v} = \left(\frac{\mathbf{z}^2 - \mathbf{zh}}{2\eta}\right)\frac{\partial \mathrm{p}}{\partial \mathbf{y}} + (\mathbf{v}_1 - \mathbf{v}_2)\frac{\mathbf{z}}{\mathbf{h}} + \mathbf{v}_2 \tag{3.18}$$

The three separate terms in any of the velocity equations (3.17) and (3.18) represent the velocity profiles across the fluid film and they are schematically shown in Fig.5

3.2.2 Continuity of Flow in a Column

Consider a column of lubricant as shown in Figure 6. The lubricant flows into the column horizontally at rates of ' $\mathbf{q}_x'$ and ' $q_y{}'$ and out of the column at rates of $\left(q_x + \frac{\partial q_x}{\partial x}dx\right)$ and $\left(\mathrm{q_y} + \frac{\partial \mathrm{q_y}}{\partial \mathrm{y}}\mathrm{dy}\right)$ per unit length and width, respectively.

In the vertical direction the lubricant flows into the column at the rate of ' $w_0\mathrm{dxdy}'$ and out of the column at the rate of ' $w_h dx dy'$, where $'\mathbf{w}_0'$ is the velocity at which the bottom of the column moves up and ' $\mathbf{w}_\mathrm{h}''$ is the velocity at which the top of the column moves up.

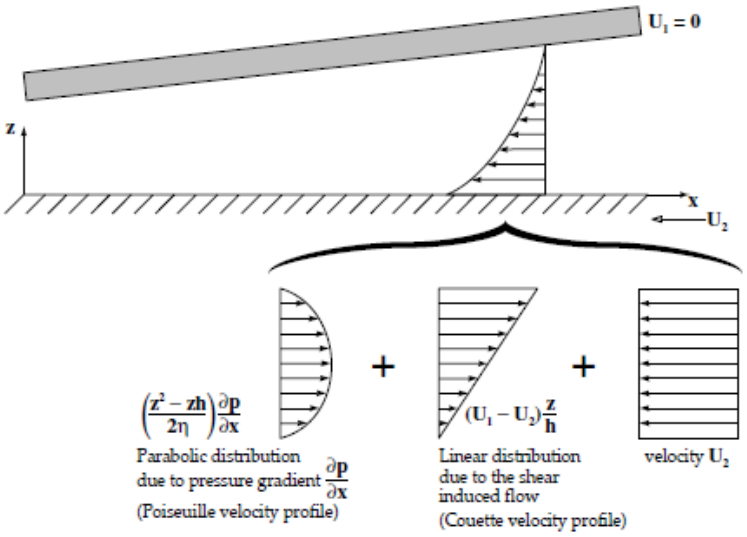

Figure 5: Velocity profiles at the entry of the hydrodynamic film. [12]

The principle of continuity of flow requires that the influx of a liquid must equal its efflux from a control volume under steady conditions.

If the density of the lubricant is constant then the following relation applies:

$$q_x dy + q_y dx + w_o dxdy = \left(q_x + \frac{\partial q_x}{\partial x} dx\right) dy + \left(q_y + \frac{\partial g_y}{\partial y} dy\right) dx + w_d dxdy \qquad (3.19)$$

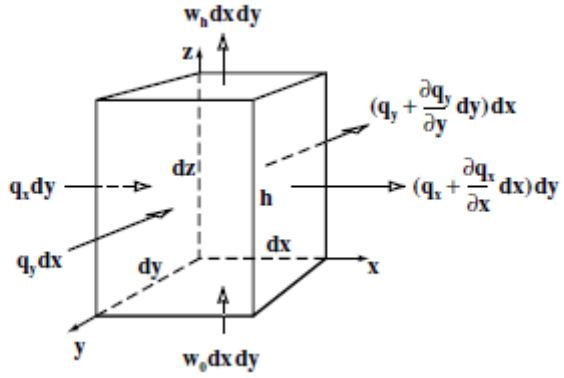

Figure 6: Continuity of flow in a column

simplifying:

$$\frac{\partial q_x}{\partial x} dxdy + \frac{\partial q_y}{\partial y} dxdy + (w_h - w_0)\, dxdy = 0 \qquad (3.20)$$

Since ' dxdy $\neq 0$ ' equation (3.20) can be rewritten as:

$$\frac{\partial \mathbf{q}_x}{\partial \mathbf{x}} + \frac{\partial \mathbf{q}_y}{\partial \mathbf{y}} + (\mathbf{w}_h - \mathbf{w}_0) = \mathbf{0} \qquad (3.21)$$

which is the equation of continuity of flow in a column.

Flow rates per unit length, ' $\mathbf{q}'_x$ and ' $\mathbf{q}_y{}'$, can be found from integrating the lubricant velocity profile over the film thickness, i.e.:

$$\mathrm{q_x} = \int_0^{\mathrm{h}} \mathrm{udz} \mathrm{q_y} = \int_0^{\mathrm{h}} \mathrm{vdz} \tag{3.22}$$

and substituting for ' $\mathbf{u}'$ from equation (3.17) yields:

$$q_x = \left| \left(\frac{x^3}{3} - \frac{z^2 h}{2} \right) \frac{\partial p}{2\eta \partial x} + (U_1 - u_2) \frac{z^2}{2h} + u_2 z \right|_0 \tag{3.23}$$

which after simplifying gives the flow rate in the ' $\mathbf{x}$ ' direction,

$$\mathrm{q_x} = -\frac{\mathrm{h}^3}{12\eta} \frac{\partial \mathrm{p}}{\partial \mathrm{x}} + (\mathrm{U}_1 + \mathrm{U}_2) \frac{\mathrm{h}}{2} \tag{3.24}$$

Similarly the flow rate in the ' y' direction is found by substituting for $'\mathbf{v}'$ from equation (3.18):

$$\mathrm{q_y} = -\frac{\mathrm{h}^3}{12\eta} \frac{\partial \mathrm{p}}{\partial \mathrm{y}} + (\mathrm{V}_1 + \mathrm{v}_2) \frac{\mathrm{h}}{2} \tag{3.25}$$

Substituting now for flow rates into the continuity of flow equation (3.21):

$$\frac{\partial}{\partial \mathrm{x}} \left[-\frac{\mathrm{h}^3}{12\eta} \frac{\partial \mathrm{p}}{\partial \mathrm{x}} + (\mathrm{U}_1 + \mathrm{U}_2) \frac{\mathrm{h}}{2} \right] + \frac{\partial}{\partial \mathrm{y}} \left[-\frac{\mathrm{h}^3}{12\eta} \frac{\partial \mathrm{p}}{\partial \mathrm{y}} + (\mathrm{V}_1 + \mathrm{v}_2) \frac{\mathrm{h}}{2} \right] + (\mathrm{w_h} - \mathrm{w_0}) = 0 \tag{3.26}$$

Defining

$$\mathrm{U} = \mathrm{U}_1 + \mathrm{U}_2 \tag{3.27}$$

and

$$\mathrm{V} = \mathrm{V}_1 + \mathrm{V}_2 \tag{3.28}$$

and assuming that there is no local variation in surface velocity in the ' x ' and ' y ' directions (i.e.,

$$\mathrm{U} \neq \mathrm{f(x)} \tag{3.29}$$

and

$$\mathrm{V} \neq \mathrm{f(y)} \tag{3.30}$$

gives:

$$-\frac{\partial}{\partial \mathbf{x}} \left(\frac{\mathbf{h}^3}{12\eta} \frac{\partial \mathbf{p}}{\partial \mathbf{x}} \right) + \frac{\mathbf{U}}{2} \frac{\partial \mathbf{h}}{\partial \mathbf{x}} - \frac{\partial}{\partial \mathbf{y}} \left(\frac{\mathbf{h}^3}{12\eta} \frac{\partial \mathrm{p}}{\partial \mathbf{y}} \right) + \frac{\mathbf{v}}{2} \frac{\partial \mathbf{h}}{\partial \mathbf{y}} + (\mathbf{w_h} - \mathbf{w_0}) = \mathbf{0} \tag{3.31}$$

Further rearranging and simplifying yields the full Reynolds equation in three dimensions.

$$\frac{\partial}{\partial \mathbf{x}} \left(\frac{\mathbf{h}^3}{\eta} \frac{\partial \mathrm{p}}{\partial \mathbf{x}} \right) + \frac{\partial}{\partial \mathbf{y}} \left(\frac{\mathbf{h}^3}{\eta} \frac{\partial \mathbf{p}}{\partial \mathbf{y}} \right) = 6 \left(\mathbf{U} \frac{\partial \mathbf{h}}{\partial \mathbf{x}} + \mathbf{v} \frac{\partial \mathbf{h}}{\partial \mathbf{y}} \right) + \mathbf{12} \left(\mathbf{w}_\mathrm{h} - \mathbf{w}_0 \right) \tag{3.32}$$

3.2.3 Simplifications to the Reynolds Equation

It can be seen that the Reynolds equation in its full form is far too complex for practical engineering applications and some simplifications are required before it can conveniently be used. The following simplifications are commonly adopted in most studies:

- Unidirectional Velocity Approximation

  It is always possible to choose axes in such a way that one of the velocities is equal to zero, i.e., V = 0. There are very few engineering systems, in which, for example, a journal bearing slides along a rotating shaft.

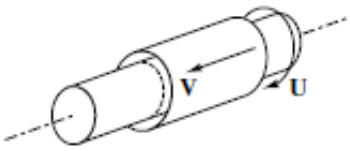

Figure 7: Unidirectional Approximation
[12]

  Assuming that V = 0, equation (3.32) can be rewritten in a more simplified form:

$$\frac{\partial}{\partial \mathbf{x}}\left(\frac{\mathbf{h}^3}{\eta}\frac{\partial \mathbf{p}}{\partial \mathbf{x}}\right)+\frac{\partial}{\partial \mathbf{y}}\left(\frac{\mathbf{h}^3}{\eta}\frac{\partial \mathbf{p}}{\partial \mathbf{y}}\right)=\mathbf{6U}\frac{\partial \mathbf{h}}{\partial \mathbf{x}}+\mathbf{12}\left(\mathrm{w_h}-\mathbf{w}_0\right) \tag{3.33}$$

- Steady Film Thickness Approximation

  It is also possible to assume that there is no vertical flow across the film i.e.

$$w_{\mathrm{h}}-\mathrm{w}_0=0 \tag{3.34}$$

  . This assumption requires that the distance between the two surfaces remains constant during the operation. Some inaccuracy may result from this analytical simplification since most bearings usually vibrate and consequently the distance between the operating surfaces cyclically varies.

  Movement of surfaces normal to the sliding velocity is known as a squeeze film effect. Furthermore, in the case of porous bearings there is always some vertical flow of oil.

  Assuming, however, that there is no vertical flow and $w_{\mathrm{h}}-w_0=0$, equation (3.33) can be written in the form:

$$\frac{\partial}{\partial \mathbf{x}}\left(\frac{\mathbf{h}^3}{\eta}\frac{\partial \mathbf{p}}{\partial \mathbf{x}}\right)+\frac{\partial}{\partial \mathbf{y}}\left(\frac{\mathbf{h}^3}{\eta}\frac{\partial \mathbf{p}}{\partial \mathbf{y}}\right)=\mathbf{6U}\frac{\partial \mathbf{h}}{\partial \mathbf{x}} \tag{3.35}$$

- Isoviscous Approximation

  For many practical engineering applications it is assumed that the lubricant viscosity is constant over the film, i.e., η = constant. This approach is known in the literature as the 'isoviscous' model where the thermal effects in hydrodynamic films

are neglected.

Assuming that η = constant, equation (3.35) can further be simplified:

$$\frac{\partial}{\partial \mathbf{x}}\left(\mathbf{h}^3\frac{\partial \mathbf{p}}{\partial \mathbf{x}}\right)+\frac{\partial}{\partial \mathbf{y}}\left(\mathbf{h}^3\frac{\partial \mathbf{p}}{\partial \mathbf{y}}\right)=\mathbf{6U}\eta\frac{\partial \mathbf{h}}{\partial \mathbf{x}} \tag{3.36}$$

- Infinitely Long Bearing Approximation

The simplified Reynolds equation (3.36) is two-dimensional and numerical methods are needed to obtain a solution.

Thus, for a simple engineering analysis further simplifying assumptions are made. It is assumed that the pressure gradient acting along the ' y' axis is negligibly small compared to the pressure gradient acting along the ' x ' axis and can be neglected, i.e., $\partial \mathbf{p}/\partial \mathrm{y} = 0$ and $\mathrm{h} \neq \mathrm{f(y)}$.

It is therefore necessary to specify that the bearing is infinitely long in the ' y′ direction. This approximation is known as the 'infinitely long bearing' or simply long bearing approximation', and is schematically illustrated in Fig.(8)

The assumption reduces the Reynolds equation to a one-dimensional form which is convenient for quick engineering analysis.

Since $\partial \mathrm{p}/\partial \mathrm{y} = 0$, the second term of the Reynolds equation (3.36) is also zero and equation (3.36) simplifies to:

$$\frac{\mathrm{d}}{\mathrm{dx}}\left(\mathrm{h}^3\frac{\mathrm{dp}}{\mathrm{dx}}\right)=6\mathrm{U}\eta\frac{\mathrm{dh}}{\mathrm{dx}} \tag{3.37}$$

which can easily be integrated, i.e.:

$$\mathrm{h}^3\frac{\mathrm{dp}}{\mathrm{dx}}=6\mathrm{U}\eta\mathrm{h}+\mathrm{C} \tag{3.38}$$

Now a boundary condition is needed to solve this equation and it is assumed that at some point along the film, pressure is at a maximum. At this point the pressure gradient is zero, i.e., $\mathrm{dp/dx} = 0$ and the corresponding film thickness is denoted as $\overline{\mathrm{h}}$.

Thus the boundary condition is:

$$\frac{dp}{dx}=0 \quad \text{at} \quad h=\bar{h} \tag{3.39}$$

Substituting to equation (3.38) gives:

$$\mathbf{C}=-\mathbf{6U}\eta\overline{\mathbf{h}} \tag{3.40}$$

and the final form of the one-dimensional Reynolds equation for the 'long bearing approximation' is:

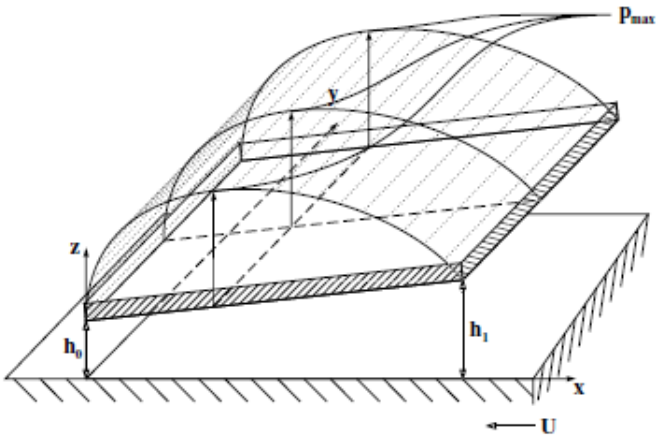

Figure 8: Pressure distribution in the long bearing approximation [12]

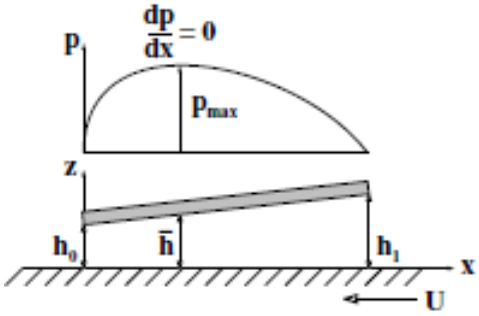

Figure 9: Pressure distribution for Linear Pad bearing [12]

$$\frac{dp}{dx} = 6\mathrm{U}\eta\frac{h-\bar{h}}{h^3} \tag{3.41}$$

which is particularly useful in the analysis of linear pad bearings. Note that the velocity 'U' in the convention assumed is negative.

Bearing Parameters Predicted from Reynolds Equation

From the Reynolds equation most of the critical bearing design parameters such as pressure distribution, load capacity, friction force, coefficient of friction and oil flow are obtained by simple integration.

Pressure Distribution

By integrating the Reynolds equation over a specific film shape described by a function h = f(x, y) the pressure distribution in the hydrodynamic lubricating film is found in terms of bearing geometry, lubricant viscosity and speed.

Load Capacity

When the pressure distribution is integrated over the bearing area the corresponding load capacity of the lubricating film is found.

If the load is varied then the film geometry will change to re-equilibrate the load and pressure field. The load that the bearing will support at a particular film geometry is:

$$W = \int_0^L \int_0^B p dx dy \tag{3.42}$$

The obtained load formula is expressed in terms of bearing geometry, lubricant viscosity and speed, hence the bearing operating and design parameters can be optimized to give the best performance.

Friction Force

Assuming that the friction force results only from shearing of the fluid and integrating the shear stress ' τ' over the whole bearing area yields the total friction force operating across the hydrodynamic film, i.e.:

$$\mathbf{F} = \int_0^{\mathrm{L}} \int_0^{\mathrm{B}} \tau \mathrm{dxdy} \tag{3.43}$$

The shear stress ' τ' is expressed in terms of dynamic viscosity and shear rates:

$$\tau = \eta \frac{\partial \mathbf{u}}{\partial \mathbf{z}} \tag{3.44}$$

where $\partial \mathbf{u}/\partial \mathrm{z}$ is obtained by differentiating the velocity equation (3.17).

After substituting for ' τ' and integrating, the formula, expressed in terms of bearing geometry, lubricant viscosity and speed for friction force per unit length, is obtained.

$$\frac{\mathrm{F}}{\mathrm{L}} = -\int_0^{\mathrm{B}} \frac{\mathrm{h}}{2} \frac{\partial \mathrm{p}}{\partial \mathrm{x}} \mathrm{dx} - \int_0^{\mathrm{B}} \frac{\mathrm{U}\eta}{\mathrm{h}} \mathrm{dx} \tag{3.45}$$

$'+'$ and $'-$ refer to the upper and lower surface, respectively. The ' $\pm$ ' sign before the first term may cause some confusion as it appears that the friction force acting on the upper and the lower surface is different which apparently conflicts with the law of equal action and reaction forces. The balance of forces becomes much clearer when a closer inspection is made of the force distribution on the upper surface as schematically illustrated in Fig. 10.

It can be seen from Fig. 10 that the reaction force from the pressure field acts in the direction normal to the inclined surface while a load is applied vertically.

Since the load is at an angle to the normal there is a resulting component 'W$tan\alpha$' acting in the opposite direction from the velocity. This is in fact the exact amount by which the frictional force acting on the upper surface is smaller than the force

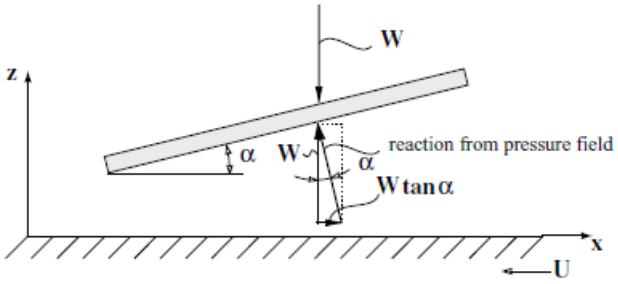

Figure 10: Load components acting on a hydrodynamic bearing. [12]

acting on the lower surface.

Coefficient of Friction

The coefficient of friction is calculated from the load and friction forces:

$$\mu = \frac{F}{W} = \frac{\int_0^L \int_0^B \tau dx dy}{\int_0^L \int_0^B p dx dy} \tag{3.46}$$

Bearing parameters can then be optimized to give, for example, a minimum value of the coefficient of friction. This means, in approximate terms, minimizing the size of the bearing by allowing the highest possible hydrodynamic pressure.
Lubricant Flow

By integrating the flow expressions $'q'_x$ and $'q'_y$, (3.24) and (3.25) over the edges of the bearing, lubricant leakage out of the sides and ends of the bearing is found.

$$\begin{aligned} Q_x &= \int_0^L q_x dy \\ Q_y &= \int_0^B q_y dx \end{aligned} \tag{3.47}$$

Lubricant flow is important to the operation of a bearing since enough oil must be supplied to the hydrodynamic contact to prevent starvation and consequent failure. The flow formulae are expressed in terms of bearing parameters and the lubricant flow can also be optimized.[1]

3.3 Newton's Method

Newton's method is root-finding algorithm. It is one of the most powerful and widely-used methods of solving f(x)=0. It originates from the Taylor series expansion of f(x) about the point x.

Starting with an initial guess x_0, we can find the value of $f(x_0)$ then approximate the graph of f by suitable tangents. With the approximate value x_0 got from the graph of f,

[1]The contents of the section 3.2 are referenced from the book "Engineering Tribology Third Edition" by STACHOWIAK, Gwidon W., Andrew BATCHELOR. which is also listed in the Bibliography section[12]

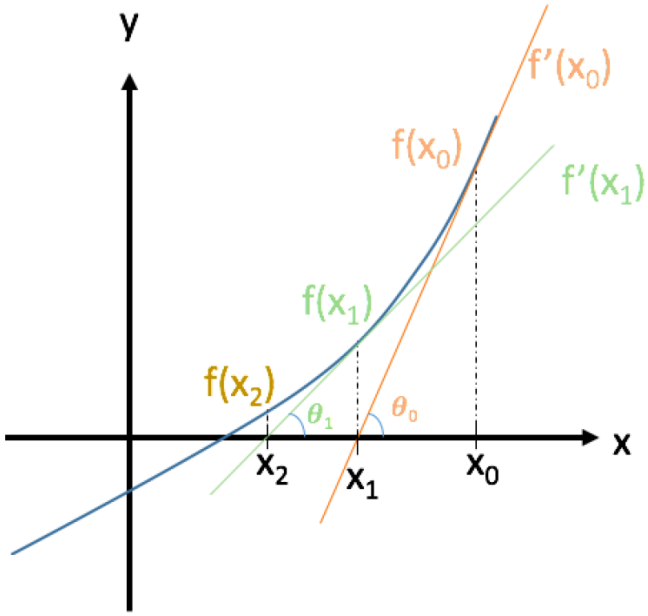

Figure 11: Newton-Raphson Method
[13]

x_1 being the intersection of the x-axis and the tangent of the curve of f at x_0.

$$\begin{aligned} \tan\theta_0 = f'(x_0) = \frac{f(x_0)}{x_0 - x_1} \\ \Rightarrow x_1 = x_0 - \frac{f(x_0)}{f'(x_0)} \end{aligned} \tag{3.48}$$

From this the Newton iteration formula can be written in the form:

$$x_{n+1} = x_n - \frac{f(x_n)}{f'(x_n)} \tag{3.49}$$

It is worthy to note that the Newton's method has some drawbacks in finding the derivative terms . This led Leong et al [14] to present the possibility of using the Jacobian while using Newton's method.

3.4 Mathematical description of the Lubricating gap

3.4.1 Bearing Pad

Pad bearings, which consist of a pad sliding over a smooth surface, are widely used in machinery to sustain thrust loads from shafts, e.g., from the propeller shaft in a ship. An example of this application is shown in Fig.(12)).

The simple film geometry of these bearings, as compared to journal bearings, renders them a suitable example for introducing hydrodynamic bearing analysis.

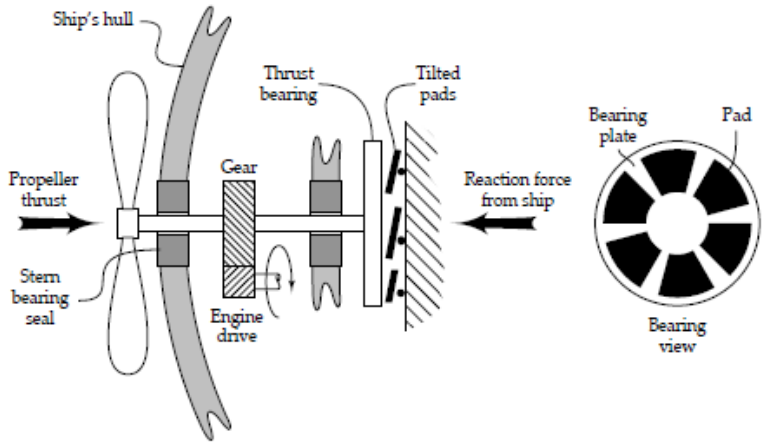

Figure 12: Example of a pad bearing application to sustain the thrust loads from the ship propeller shaft.

[12]

Infinite Linear Pad Bearing

The infinite linear pad bearing, as already mentioned, is a pad bearing of infinite length normal to the direction of sliding. This particular bearing geometry is the easiest to analyse.

Consider an infinitely long linear wedge with $L/B > 3$ as shown in Fig.(13), where ' L ' and B′ are the pad dimensions normal to and parallel to the sliding direction, i.e., pad length and width, respectively.

Assume that the bottom surface is moving in the direction shown, dragging the lubricant into the wedge which results in pressurization of the lubricant within the wedge. The inlet and the outlet conditions of the wedge are controlled by the maximum and minimum film thicknesses, $'\mathbf{h}'_1$ and $'\mathbf{h}'_0$, respectively.

Bearing Geometry

The bearing geometry of a journal bearing is formed when the journal center location is non-concentric in the bearing. The journal rotation drags oil into the wedge and generates pressure which then separates the sliding pair[**?**].

As a first step in any bearing analysis the bearing geometry, i.e, $\mathbf{h}$ = f(x), must be defined. The film thickness $\mathbf{h}'$ in Figure 4.9 is expressed as a function:

$$h = h_0 + x \tan \alpha = h_0 + x \frac{h_1 - h_0}{B} \tag{3.50}$$

or simply:

$$h = h_0 \left(1 + \frac{h_1 - h_0}{h_0} \frac{x}{B} \right) \tag{3.51}$$

The term $(\mathrm{h}_1 - \mathrm{h}_0)/\mathrm{h}_0$ is often known as the convergence ratio K′[3, 4]. The film

geometry can then be expressed as:

$$h = h_0 \left(1 + \frac{Kx}{B}\right) \tag{3.52}$$

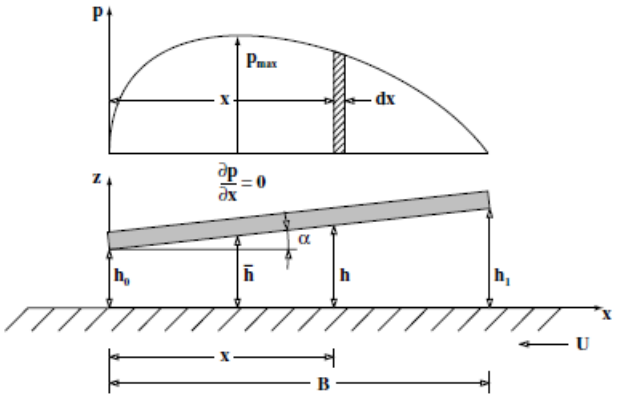

Figure 13: Geometry of a linear pad bearing.
[12]

Number of bearing pads

The number of pads in the thrust bearing of the turbocharger is given by:

$$\phi_0 = 2\pi/n_p \tag{3.53}$$

It is given in the initial problem that $\phi_0 = 60°$

The number of bearing pads,

$$n_p = 6 \tag{3.54}$$

3.4.2 Bearing Analysis

The thrust bearing design is complicated. Complete analysis requires consideration of heat generation, oil flow, bearing material, load capacity, and stiffness.

For the problem being considered, analysis would consider load capacity, friction force and oil flow rate.

Pressure Distribution

As mentioned already, the pressure distribution can be calculated by integrating the Reynolds equation over the specific film geometry. Since the pressure gradient in the ${}^{i}\mathrm{x}'$ direction is dominant, the one-dimensional Reynolds equation for the long bearing approximation (3.41) can be used for the analysis of this bearing:

$$\frac{\mathrm{d}p}{\mathrm{dx}} = 6\mathrm{U}\eta\frac{\mathrm{h}-\overline{\mathrm{h}}}{\mathrm{h}^3}$$

There are two variables, $'\mathbf{x}'$ and $'\mathbf{h}'$, and the equation can be integrated with respect to $'\mathrm{x}'$ or $'h'$. Since it does not really matter with respect to which variable the integration is performed we choose ' h'. Firstly one variable is replaced by the other.

This can be achieved by differentiating (3.52) which gives $'\mathrm{d}x'$ in terms of ' dh''

$$\mathrm{dx} = \frac{\mathrm{B}}{\mathrm{Kh_p}}\mathrm{dh} \tag{3.55}$$

Substituting into (3.41) yields:

$$\frac{dp}{\frac{B}{Kh_0}dh} = 6U\eta\frac{h-\bar{h}}{h^3} \tag{3.56}$$

and after simplifying and separating variables:

$$\frac{\mathbf{Kh_0}}{\mathbf{6U}\eta\mathbf{B}}\mathbf{dp} = \frac{\mathbf{h}-\overline{\mathbf{h}}}{\mathrm{h}^3}\mathrm{dh} \tag{3.57}$$

which is the differential formula for pressure distribution in this bearing. Equation (3.57) can be integrated to give:

$$\frac{\mathrm{Kh_0}}{6\mathrm{U}\eta\mathrm{B}}\mathrm{p} = -\frac{1}{\mathrm{h}} + \frac{\overline{\mathrm{h}}}{2\ \mathrm{h}^2} + \mathrm{C} \tag{3.58}$$

The boundary conditions, taken from the bearing's inlet and outlet, are (Fig. 13):

$$\begin{aligned} \mathrm{p} &= \mathbf{0} \quad \text{at} \quad \mathrm{h} = \mathrm{h_0} \\ \mathrm{p} &= \mathbf{0} \quad \text{at} \quad \mathrm{h} = \mathrm{h_1} \end{aligned} \tag{3.59}$$

Substituting into (3.58) the constants $\bar{h}'$ and ${}^{s}\mathbf{C}'$ are:

$$\overline{\mathbf{h}} = \frac{2\mathbf{h_1}\mathbf{h_1}}{\mathbf{h_1}+\mathbf{h_1}} \tag{3.60}$$

$$\mathrm{C} = \frac{1}{\mathrm{h_1}+\mathrm{h_0}} \tag{3.61}$$

The maximum film thickness $'\mathbf{h}_1'$, can also be expressed in terms of the convergence ratio $'\mathbf{K}'$:

$$\mathbf{K} = \frac{\mathbf{h_1}-\mathbf{h_0}}{\mathbf{h_0}} \tag{3.62}$$

Thus:

$$\mathbf{h_1} = \mathbf{h_0}(\mathbf{K}+\mathbf{1}) \tag{3.63}$$

Substituting into (3.61) the constants $\bar{h}'$ and ' C' in terms of $'K'$ are:

$$\begin{aligned} \overline{\mathrm{h}} &= 2\ \mathrm{h}_0 \frac{(\mathbf{K}+\mathbf{1})}{(\mathbf{K}+2)} \\ \mathrm{C} &= \frac{1}{\mathrm{h}_0(\ \mathrm{K}+2)} \end{aligned} \tag{3.64}$$

Substituting into (3.58) gives:

$$\frac{\mathbf{K}\mathbf{h}_0}{\mathbf{6}\mathbf{U}\eta\mathbf{B}}\mathbf{p} = -\frac{\mathbf{1}}{\mathbf{h}} + \frac{\mathbf{h}_0}{\mathbf{h}^2}\frac{(\mathbf{K}+\mathbf{1})}{(\mathbf{K}+2)} + \frac{\mathbf{1}}{\mathbf{h}_0(\mathbf{K}+\mathbf{2})} \tag{3.65}$$

or:

$$\mathrm{p} = \frac{\mathbf{6}\mathbf{U}\eta\mathbf{B}}{\mathrm{K}\mathrm{h}_0}\left(-\frac{1}{\mathrm{h}} + \frac{\mathrm{h}_0}{\mathrm{h}^2}\frac{(\mathbf{K}+\mathbf{1})}{(\mathrm{K}+2)} + \frac{1}{\mathrm{h}_0(\ \mathrm{K}+2)}\right) \tag{3.66}$$

It is useful to find the pressure distribution in the bearing expressed in terms of bearing geometry and operating parameters such as the velocity ' U′ and lubricant viscosity ' η'.
A convenient method of finding the controlling influence of these parameters is to introduce non-dimensional parameters. In bearing analysis non-dimensional parameters such as pressure and load are used. Equation (3.66) can be expressed in terms of a nondimensional pressure, i.e.:

$$\mathrm{p}^* = \frac{\mathrm{h}_0}{\mathrm{K}}\left(-\frac{1}{\mathrm{h}} + \frac{\mathrm{h}_0}{\mathrm{h}^2}\frac{(\mathrm{K}+1)}{(\mathrm{K}+2)} + \frac{1}{\mathrm{h}_0(\ \mathrm{K}+2)}\right) \tag{3.67}$$

where the non-dimensional pressure ' $\mathbf{p}^{\star\prime}$ is:

$$\mathbf{p}^* = \frac{{\mathbf{h}_0}^2}{\mathbf{6}\mathbf{U}\eta\mathrm{B}}\mathbf{p} \tag{3.68}$$

It is clear that hydrodynamic pressure is proportional to sliding speed ' U′ and bearing width ′B′ for a given value of dimensionless pressure and proportional to the reciprocal of film thickness squared.
If a quick estimate of hydrodynamic pressure is required to check, for example, whether the pad material will suffer plastic deformation, a representative value of dimensionless pressure can be multiplied by the selected values of sliding speed, viscosity and bearing dimensions to yield the necessary information.

- *Load Capacity*

  The total load that a bearing will support at a specific film geometry is obtained by integrating the pressure distribution over the specific bearing area.

$$\mathbf{W} = \int_0^{\mathrm{L}}\int_0^{\mathrm{B}} \mathrm{pdxdy} \tag{3.69}$$

  This can be re-written in terms of load per unit length:

$$\frac{\mathbf{W}}{\mathbf{L}} = \int_0^{\mathrm{B}} \mathrm{pdx} \tag{3.70}$$

  and substituting for ' p′, equation (3.66), yields:

$$\frac{\mathbf{W}}{\mathrm{L}} = \frac{6\mathrm{U}\eta\mathrm{B}}{\mathrm{K}\mathrm{h}_0}\int_0^{\mathrm{n}}\left(-\frac{1}{\mathrm{h}} + \frac{\mathrm{h}_0}{\mathrm{h}^2}\frac{(\mathrm{K}+1)}{(\mathrm{K}+2)} + \frac{1}{\mathrm{h}_0(\ \mathrm{K}+2)}\right)\mathrm{dx} \tag{3.71}$$

Again there are two variables in (3.71), $'\mathbf{x}'$ and $\mathbf{h}'$, and one has to be replaced by the other before the integration can be performed. Substituting (3.55) for $'\mathrm{d}\mathbf{x}'$, and integrating yields:

$$\frac{\mathbf{W}}{\mathbf{L}} = \frac{\mathbf{6U}\eta\mathbf{B}^2}{\mathbf{K}^2{\mathbf{h}_0}^2}\left(-\ln(\mathbf{K}+\mathbf{1}) + \frac{\mathbf{2K}}{\mathbf{K}+2}\right) \tag{3.72}$$

Equation (4.2) is the total load per unit length the bearing will support, expressed in terms of the bearing's geometrical and operating parameters. In terms of the non-dimensional load $'\ \mathrm{W}^{*\prime}$, equation (4.2) can be expressed as:

$$\mathbf{W}^* = \frac{\mathbf{1}}{\mathbf{K}^2}\left(-\ln(\mathbf{K}+\mathbf{1}) + \frac{\mathbf{2K}}{\mathbf{K}+\mathbf{2}}\right) \tag{3.73}$$

where:

$$\mathbf{W}^* = \frac{{\mathbf{h}_0}^2}{6\mathrm{U}\eta\mathrm{B}^2\ \mathrm{L}}\mathbf{W} \tag{3.74}$$

- *Friction Force*

The friction force generated in the bearing due to the shearing of the lubricant is obtained by integrating the shear stress $'\ \tau'$ over the bearing area (equation 3.43):

$$\mathbf{F} = \int_0^{\mathrm{L}}\int_0^{\mathrm{B}}\tau\mathrm{dxd}\mathbf{y} \tag{3.75}$$

The friction force per unit length is:

$$\frac{\mathbf{F}}{\mathbf{L}} = \int_0^{\mathrm{B}}\tau\mathrm{dx} \tag{3.76}$$

As already mentioned, shear stress is defined in terms of dynamic viscosity and shear rate:

$$\tau = \eta\frac{\partial\mathbf{u}}{\partial\mathbf{z}} \tag{3.77}$$

where $\partial\mathbf{u}/\partial\mathrm{z}$ is obtained by differentiating the velocity equation (3.17). In the bearing considered, the bottom surface is moving while the top surface remains stationary, i.e.:

$$\mathbf{U}_1 = \mathbf{0} \text{ and } \mathbf{U}_2 = \mathbf{U} \tag{3.78}$$

thus the velocity equation (3.17) is:

$$\mathbf{u} = \left(\frac{\mathbf{z}^2 - \mathbf{zh}}{2\eta}\right)\frac{\partial\mathbf{p}}{\partial\mathbf{x}} - \mathbf{U}\frac{\mathbf{z}}{\mathbf{h}} + \mathbf{U} \tag{3.79}$$

Differentiating gives the shear rate:

$$\frac{\partial\mathbf{u}}{\partial\mathbf{z}} = (\mathbf{2z} - \mathbf{h})\frac{\mathbf{1}}{2\eta}\frac{\mathrm{d}\mathbf{p}}{\mathbf{dx}} - \frac{\mathrm{U}}{\mathbf{h}} \tag{3.80}$$

and substituting yields the friction force per unit length:

$$\frac{\mathbf{F}}{\mathrm{L}} = \int_0^{\mathrm{B}} \left[\left(\mathrm{z} - \frac{\mathrm{h}}{2} \right) \frac{\mathrm{dp}}{\mathrm{dx}} - \frac{\mathrm{U}\eta}{\mathrm{h}} \right] \mathrm{dx} \tag{3.81}$$

The friction force on the lower moving surface, as explained already, is greater than on the upper stationary surface. At the moving surface z = 0 (as shown in Fig. 13), hence the acting frictional force per unit length is:

$$\frac{\mathrm{F}}{\mathrm{L}} = \int_0^{\mathrm{B}} \left(-\frac{\mathrm{h}}{2}\frac{\mathrm{dp}}{\mathrm{dx}} - \frac{\mathrm{U}\eta}{\mathrm{h}} \right) \mathrm{dx} \tag{3.82}$$

or:

$$\frac{\mathbf{F}}{\mathrm{L}} = -\int_0^{\mathrm{B}} \frac{\mathrm{h}}{2}\frac{\mathrm{dp}}{\mathrm{dx}}\mathrm{dx} - \int_0^{\mathrm{E}} \frac{\mathrm{U}\eta}{\mathrm{h}}\mathrm{dx} \tag{3.83}$$

The first part of the above equation must be integrated by parts. According to the theorems of integration, the general mathematical formula to integrate by parts is:

$$\int \mathrm{adb} = \mathrm{ab} - \int \mathrm{bda} \tag{3.84}$$

So if,

$$\mathrm{a} = \frac{\mathrm{h}}{2} \quad \text{and} \quad \mathrm{db} = \frac{\mathrm{dp}}{\mathrm{dx}}\mathrm{dx} \tag{3.85}$$

then:

$$da = \frac{1}{2}dh \quad \text{and} \quad b = \int \frac{dp}{dx}dx = p \tag{3.86}$$

substituting:

$$-\int_0^B \frac{h}{2}\frac{dp}{dx}dx = -\left(\left| \frac{h}{2}p \right|_0^n - \int_0^B \frac{1}{2}pdh \right) \tag{3.87}$$

Since p = 0 at x = 0 and at x = B (Fig. 13) the term $| \frac{\mathrm{h_2p}}{\mathrm{p}}$ also equals zero.

In the remaining term variables are replaced before integration and substituting for ' dh ' (equation (3.55)) gives:

$$-\int_0^{\mathrm{B}} \frac{\mathrm{h}}{2}\frac{\mathrm{dp}}{\mathrm{dx}}\mathrm{dx} = 0 + \int_0^{\mathrm{B}} \frac{1}{2}\mathrm{p}\frac{\mathrm{Kh_0}}{\mathrm{B}}\mathrm{dx} = \frac{\mathrm{Kh_0}}{2\ \mathrm{B}}\int_0^{\mathrm{B}} \mathrm{pdx} \tag{3.88}$$

Thus the first term of equation (3.83) is:

$$-\int_0^{\mathrm{B}} \frac{\mathrm{h}}{2}\frac{\mathrm{dp}}{\mathrm{dx}}\mathrm{dx} = \frac{\mathrm{Kh_0}}{2\ \mathrm{B}}\frac{\mathrm{w}}{\mathrm{L}} \tag{3.89}$$

Integrating the second term of equation (3.83):

$$\int_0^{\mathrm{B}} \frac{\mathrm{U}\eta}{\mathrm{h}}\mathrm{dx} = \int_0^{\mathrm{B}} \frac{\mathrm{U}\eta}{\mathrm{h_0}\left(1 + \frac{\mathrm{Kx}}{\mathrm{B}}\right)}\mathrm{dx} = \frac{\mathrm{U}\eta}{\mathrm{h_0}}\int_0^{\mathrm{B}} \frac{\mathrm{dx}}{\left(1 + \frac{\mathrm{Kx}}{\mathrm{B}}\right)} \tag{3.90}$$

hence:

$$\int_0^{\mathrm{B}} \frac{\mathrm{U}\eta}{\mathrm{h}}\mathrm{dx} = \frac{\mathrm{U}\eta\mathrm{B}}{\mathrm{h_0\ K}}\ln(1 + \mathrm{K}) \tag{3.91}$$

Substituting (3.89) and (3.91) into (3.83), the expression for friction force per unit length for a linear pad bearing is obtained:

$$\frac{\mathbf{F}}{\mathbf{L}} = \frac{\mathbf{K h_0}}{2\ \mathrm{B}} \frac{\mathbf{W}}{\mathrm{L}} - \frac{\mathrm{U}\eta\mathrm{B}}{\mathrm{h_0\ K}} \ln(1 + \mathbf{K}) \tag{3.92}$$

Note that calculating the friction force for the upper surface, i.e., for z = h, and subtracting from equation (3.92) yields $\mathrm{Kh_0\ W/BL} = \mathrm{W} \tan\alpha/\mathrm{L}$.

Substituting for W′ (equation (4.2)),

$$\mathbf{W} = \frac{6\mathrm{U}\eta\mathrm{B}^2\ \mathrm{L}}{\mathrm{K}^2\ {\mathrm{h_0}}^2} \left(- \ln(\mathrm{K} + 1) + \frac{2\ \mathrm{K}}{\mathrm{K} + 2} \right) \tag{3.93}$$

and simplifying:

$$\frac{\mathbf{F}}{\mathbf{L}} = \frac{\mathbf{U}\eta\mathbf{B}}{\mathbf{h_0}} \left(\frac{6}{\mathbf{K} + 2} - \frac{4 \ln(\mathbf{K} + 1)}{\mathbf{K}} \right) \tag{3.94}$$

In a similar manner to load and pressure, frictional force is expressed in terms of the bearing's geometrical and operating parameters. In terms of the non-dimensional friction force $'\mathrm{F}^\star$ equation (4.3) is given by:

$$\mathrm{F}^* = \frac{6}{\mathbf{K} + 2} - \frac{4 \ln(\mathrm{K} + 1)}{\mathrm{K}} \tag{3.95}$$

where:

$$\mathbf{F}^* = \frac{\mathbf{h_0}}{\mathbf{U}\eta\mathbf{BL}}\mathbf{F} \tag{3.96}$$

The bearing geometry can now be optimized to give a minimum friction force, but it is more useful to optimize the bearing to find the minimum coefficient of friction since this provides the most efficient bearing geometry for any imposed load.

- *Coefficient of Friction*

By definition the coefficient of friction is expressed as a ratio of the friction and normal forces acting on the surface:

$$\mu = \frac{\mathbf{F}}{\mathbf{W}} = \frac{\mathbf{F/L}}{\mathbf{W/L}} \tag{3.97}$$

substituting for F/L and W/L and simplifying:

$$\mu = \frac{\mathbf{K h_0}}{\mathbf{B}} \left[\frac{3\ \mathrm{K} - 2(\mathbf{K} + 2) \ln(\mathbf{K} + \mathbf{1})}{6\ \mathrm{K} - 3(\mathbf{K} + 2) \ln(\mathbf{K} + \mathbf{1})} \right] \tag{3.98}$$

As was performed with load and friction, ' μ ' can also be expressed in a so-called nondimensional or normalized form. In precise terms $'\mu'$ is already non-dimensional but the purpose here is to find a general parameter which is independent of basic bearing characteristics such as load and size. Therefore ' μ' is defined entirely in terms of other nondimensional parameters:

$$\mu^* = \mathbf{K}\left[\frac{3\ \mathrm{K} - 2(\mathbf{K}+2)\ln(\mathbf{K}+\mathbf{1})}{6\ \mathrm{K} - 3(\mathbf{K}+2)\ln(\mathbf{K}+\mathbf{1})}\right] \tag{3.99}$$

where:

$$\mu^* = \frac{B}{h_0}\mu \tag{3.100}$$

- *Lubricant flow rate*

Lubricant flow rate is an important design parameter. Sufficient quantity of lubricant must be supplied to the bearing to fully separate the surfaces by a hydrodynamic film. If the quantity of lubricant is supplied is in excess, then secondary frictional losses such as churning of the lubricant become significant. This effect can even overweigh the direct bearing frictional power loss. Precise calculation of lubricant flow is necessary to prevent overheating of the bearing from either lack of lubricant or excessive churning [12].

$$\mathrm{q_y} = 0 \tag{3.101}$$

Hence the lubricant flow in the bearing is obtained by integrating the flow per unit length $'\mathrm{q}'_\mathrm{x}$ over the length of the bearing:

$$\mathrm{Q_r} = \int_0^\mathrm{L} \mathrm{q}_x\ \mathrm{dy} \tag{3.102}$$

We know, from the equations describing the flow in a column that the flow rate in the x-direction is given by:

$$\mathrm{q_x} = -\frac{\mathrm{h}^3}{12\eta}\frac{\partial \mathrm{p}}{\partial \mathrm{x}} + (\mathbf{U}_1 + \mathbf{U}_2)\frac{\mathrm{h}}{2} \tag{3.103}$$

Substituting for ' $\mathbf{q}'_\mathrm{x}$ in the above equation :

$$\mathrm{Q_x} = \int_0^\mathrm{L}\left(-\frac{\mathrm{h}^3}{12\eta}\frac{\partial \mathrm{p}}{\partial \mathrm{x}} + \frac{\mathrm{Uh}}{2}\right)\mathrm{dy} \tag{3.104}$$

The boundary conditions shown in Fig. 13 are:

$$\frac{dp}{dx} = 0 \tag{3.105}$$

at h=$\bar{h}$ (point of maximum pressure)

substituting into equation(3.105) the flow is:

$$\mathbf{Q_x} = \int_0^\mathrm{L} \frac{\mathbf{U}\overline{\mathbf{h}}}{\mathbf{2}}\mathbf{dy} \tag{3.106}$$

substituting for $\overline{\mathrm{h}}'$ (equation 3.64):

$$\mathbf{Q_x} = \int_0^\mathbf{L} \frac{\mathbf{U}}{\mathbf{2}}\mathbf{2h}_0\left(\frac{\mathbf{K}+\mathbf{1}}{\mathbf{K}+\mathbf{2}}\right)\mathbf{dy} \tag{3.107}$$

and simplifying yields the lubricant flow per unit length: [2]

$$\frac{Q_{\mathrm{J}}}{\mathrm{L}} = \mathrm{U}h_0 \left(\frac{\mathbf{K}+\mathbf{1}}{\mathbf{K}+2} \right) \tag{3.108}$$

3.4.3 Generalized Gap Profile

General Gap Profile

The general gap profile is described by a piecewise linear function.

It was chosen by discretizing a variation of the analytical profile described by equation (3.51) ands five control points were introduced.

$$h = h_0 \left(1 + \frac{h_1 - h_0}{h_0} \frac{x}{B} \right) \tag{3.109}$$

In this case, the general gap profile shape can be varied by changing any of its five control points.

Shape Optimization

Shape optimization is a very integral part of design and construction. For example, if an aircraft is to be marked safe to use, there are criteria on mechanical performance it must satisfy while weighing as little as possible.

"The shape optimization problem for structures like the aircraft consists in finding a geometry of the structure which minimizes a given functional (e.g. such as the weight of the structure) and yet simultaneously satisfies specific constraints (like thickness, strain energy, or displacement bounds). The geometry of the structure can be considered as a given domain in the three-dimensional Euclidean space. The domain is an open, bounded set whose topology is given, e.g. it may be simply or doubly connected. The boundary is smooth or piecewise smooth, so boundary value problems that are defined in the domain and associated with the classical partial differential equations of mathematical physics are well posed. [15]"

Generally, the objective function (cost functional), takes the form of an integral over the domain or its boundary where the integrand depends smoothly on the solution of a boundary value problem.

The shape optimization problem then involves the minimization of such a functional with respect to the geometrical domain which must belong to the admissible family, the set of admissible solutions.

To solve a shape optimization problem is to find the minimum - whenever it exists - of a specific cost functional over a set of admissible domains. However, very few adequate

[2] The contents of the sections 3.4.2 & 3.4.1 are referenced from the book "Engineering Tribology Third Edition" by STACHOWIAK, Gwidon W., Andrew BATCHELOR. which is also listed in the Bibliography section[12]

results exist. The existence of the results for these problems are obtained, provided that some constraint, mostly unrealistic, are imposed on the family of admissible domains [15].

The process of finding the best design possible can be mathematically expressed with an objective function. In our case, it is a multi-objective function.

3.4.4 MultiObjective Optimization

The many types of multi-objective optimization problems can be solved by many methods. Some methods for solving multi-objective optimization problems include:

- **The Global Criterion Method:** which involves the use of a criterion method to transform a plural problem problem optimization into a single problem optimization. This is done by minimizing the distance between many reference points, ideal solutions, and feasible destination areas.

- **Weighted-sum method:** combines all the problems into one problem using a weighted vector. The number of weights is usually normalized to one.

- **Lexicographic Method:** where the decision makers regulate the objective function depending on absolute interests. The objectives are ranked by a predetermined order of importance. The optimization is then carried out individually on each objective by the order of importance. The result of the most important objective is most likely the optimal solution; if it has only one solution. In the event where there is not a single optimal solution, the second objective, in the order of importance, will be optimized with new constraints on the obtained solution from the first objective. The cycle continues until the last objective. [16]

In the weighted-sum method, to avoid the exclusion of any objective, each single objective can be judged through weights.

Scalarization of the MultiOjective function

If it is defined that $\lambda_1 > 0, \lambda_2 > 0, ..., \lambda_p > 0$ and the problem is considered as

$$min(\lambda_1 f_1(x) + \lambda_2 f_2(x) + ...\lambda_p f_p(x)), x \in \mathcal{S}, \tag{3.110}$$

where $\mathcal{S}$ is the set of optimal solutions.

with $\lambda_1 < \lambda_2 < ... < \lambda_p$, "importance" is given to the first objective than is given to the second, the second is ascribed more "importance" than the third, and so on. [17]

Generally multiobjective optimization problems are solved by scalarization, the replacement of a vector optimization problem with a scalar optimization problem, i.e. converting the problem into a family of single objective optimization problems with real-valued objective functions depending on some parameters.[16]

$$\min_{x\in\mathcal{X}} \sum_{k=1}^{p} \lambda_k f_k(x) \tag{3.111}$$

where λ denotes the scalar product in $\mathbb{R}^p$.

This optimization problem is called weighted sum scalarization of the multicriteria optimization problem.[17]

Nondominated points represent the image of the set of efficient points.

There exists the possibility of having many efficient solutions for a multicriteria optimization problem. Then, a final choice is to be made among these different efficient outcomes.

Suppose we want to minimize both x_1 and x_2 of a circle with a unitary ray

$$min(x_1, x_2) \tag{3.112}$$

subject to $x_1^2 + x_2^2 \geq 4$

if we minimize for $x_1 = 4$ we cannot minimize for x_2 and vice versa.

We try to find the best trade-off possible over the set of feasible alternatives.

The best solution being a solution that is strictly better in one objective without being worse in another. [17]

Let $\mathcal{Y} \subset \mathbb{R}^p$.

For a fixed $\lambda \in \mathbb{R}^p_{\leq}$ the set of optimal points of $\mathcal{Y}$ with respect to λ is given by

$$\mathcal{S}(\lambda, \mathcal{Y}) := \left\{ \hat{y} \in \mathcal{Y} : \langle \lambda, \hat{y} \rangle = \min_{y\in\mathcal{Y}} \langle \lambda, y \rangle \right\} \tag{3.113}$$

Due to the definition of nondominated points, considering only nonnegative weighting $\lambda \in \mathbb{R}^p_{\leq}$ and it is essential to make a distinction among optimal points with nonnegative and positive weights.

For this purpose, define

$$\begin{aligned} \mathcal{S}(\mathcal{Y}) &:= \bigcup_{\lambda\in\mathbb{R}^p_{>}} \mathcal{S}(\lambda, \mathcal{Y}) = \bigcup_{\left\{\lambda>0:\sum_{k=1}^{p}\lambda_k=1\right\}} \mathcal{S}(\lambda, \mathcal{Y}) \\ \text{and } \mathcal{S}_0(\mathcal{Y}) &:= \bigcup_{\lambda\in\mathbb{R}^p_{\geq}} \mathcal{S}(\lambda, \mathcal{Y}) = \bigcup_{\left\{\lambda\geq0:\sum_{k=1}^{p}\lambda_k=1\right\}} \mathcal{S}(\lambda, \mathcal{Y}) \end{aligned} \tag{3.114}$$

As a simple notation, we have

$$\begin{aligned} \Lambda &:= \left\{ \lambda \in \mathbb{R}^p_{\geq} : \sum_{k=1}^{p} \lambda_k = 1 \right\} \\ \Lambda^0 &:= \operatorname{ri} \Lambda \left\{ \lambda \in \mathbb{R}^p >: \sum_{k=1}^{p} \lambda_k = 1 \right\}. \end{aligned} \tag{3.115}$$

We exclude the case in which $\lambda = 0$.
Finally, following from the definition;

$$\mathcal{S}(\mathcal{Y}) \subset \mathcal{S}_0(\mathcal{Y}) \tag{3.116}$$

For results, there needs to be some convexity assumption; the problem is that convexity assumption on $\mathcal{Y}$ would be too restrictive. Having in mind that we are looking for nondominated points that are located in the "south-west" part of $\mathcal{Y}$, we define $\mathbb{R}^p_{\leqq}$ -convex.

Definition 3.1. A set $\mathcal{Y} \in \mathbb{R}^p_{\leqq}$ is called $\mathbb{R}^p_{\leqq}$ -convex, if $\mathcal{Y} + \mathbb{R}^p_{\leqq}$ is convex.

Every convex set $\mathcal{Y}$ is $\mathbb{R}^p_{\geq}$ -convex. A fundamental result from convex sets is that nonintersecting convex sets can be separated by a hyperplane.

Theorem 3.1. *Let $\mathcal{Y}_1, \mathcal{Y}_2 \subset \mathbb{R}^p$ be nonempty convex sets. There exists some $y^* \in \mathbb{R}^p$ such that*

$$\begin{aligned} &\inf_{y \in \mathcal{Y}_1} \langle y, y^* \rangle \geq \sup_{y \in \mathcal{Y}_2} \langle y, y^* \rangle \\ &\textit{and } \sup_{y \in \mathcal{Y}_1} \langle y, y^* \rangle > \inf_{y \in \mathcal{Y}_2} \langle y, y^* \rangle \end{aligned} \tag{3.117}$$

if and only if $\operatorname{ri}(\mathcal{Y}_1) \cap \operatorname{ri}(\mathcal{Y}_2) \neq \emptyset$. *In this case $\mathcal{Y}_1, \mathcal{Y}_2$ are properly separated by a hyperplane with normal y^*.*

where ri $(\mathcal{Y}_i)$ is the interior in the space of appropriate dimension $\dim(\mathcal{Y}_i) \leq p$.[17]

Theorem 3.2. *Let $\mathcal{Y} \subset \mathbb{R}^p$ be a nonempty, closed, convex set and let $y^0 \in \mathbb{R}^p \backslash \mathcal{Y}$. Then there exists a $y^* \in \mathbb{R}^p \backslash \{0\}$ and $\alpha \in \mathbb{R}$ such that*

$$\begin{aligned} &\left\langle y^*, y^0 \right\rangle < \alpha < \langle y^*, y \rangle \\ &\textit{for all } y \in \mathcal{Y}. \end{aligned} \tag{3.118}$$

The problem to be solved is an multi-objective optimization problem.

The criteria under which the problem is to be solved:

i Minimize friction force.

ii Maintain load capacity.

iii Do not increase lubricant flow rate.

iv Do not decrease minimum gap thickness.

For the thesis problem, the weighted-sum method was employed. This method is one method of scalarization of the objective function.

3.5 Genetic Algorithm

3.5.1 Introduction

Many problems of science are solved by imitating nature, many insights that have advanced science have come from this process. Genetic algorithm is the computational adaptation of the evolution process. Specifically, it attempts to replicate Lamarck's process of natural selection.

The genetic algorithm is a kind of evolutionary algorithm. Evolutionary algorithms first construct an initial population, then reiterates through three procedures:

i Fitness evaluation: The fitness of the individuals in the population is evaluated. Members of the population are stochastically selected based on their fitness.

ii Breeding: the selected individuals form the parent population. They then breed among themselves to produce offspring.

iii Crossover and mutation: the members of the parent population are selected randomly and modified. The offspring population is subjected to fitness evaluation and stochastically selected for breeding with each other and/or with selected members of the parent population.

Then this process is repeated until a certain condition is satisfied.

Genetic algorithms are multi-directional search, derivative-free stochastic search algorithms that apply the idea of natural selection.

One of the many difficulties in engineering design and multi-objective optimization is meeting the robustness requirement. Genetic algorithms are being extensively applied to engineering problems because they can locate pareto front. The pareto front is a set of reduced actions. It is derived after weaker solutions, solutions that are easily dominated by most other solutions in the set of solutions, have been removed or taken away from the set of solutions.

Dominance ranks are used to push the population close to the pareto front. With larger population there is the tendency to be more localized in the search for an optimal result. For a more robust solution, it is good allow for diversity. It is common knowledge that in industry, most times, robustness of solutions sometimes trump optimality. Therefore, to allow for robustness of solution and to get some 'control of the population', diversity must be adapted into this search algorithm. Though paradoxical, the goal is to

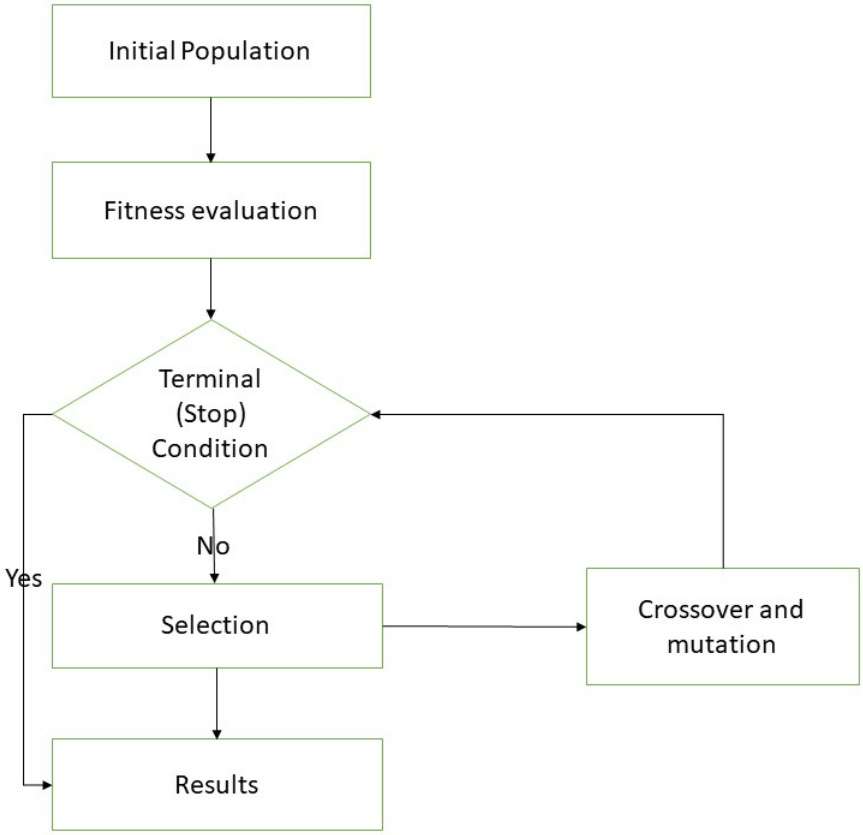

Figure 14: Flowchart for Genetic Algorithm

attain convergence and diversity.

Advantages of Genetic Algorithm

- It is robust; has a wide range of applications.
- It can be directly implemented in optimization tools and packages.
- It is easy to deal with discrete design variables.
- It is useful in finding global solution of multivariate objective function.
- It effortlessly captures multiple non-inferior solutions.
- It uses probabilistic and not deterministic operators.
- It is less likely to be trapped in a local minimum.
- Provides local and global solution.
- In many cases, they are less sensitive to the presence of noise and uncertainty in measurements.

Disadvantages of Genetic Algorithm:

- It requires comparatively less information about the problem.

- It is computationally time consuming. A single solution of a bearing steady state may include hours of computational time on high-performance computers. This fact makes it practically impossible to use these calculations for multiple repetitive tasks involving the solution of hundreds or thousands of operating states.

3.5.2 Adaptation of the Genetic Algorithm to our problem

"GA problematics use standard terminology: an individual, a gener- ation, a gene, an objective function or a fitness function. Thrust bear- ing integral characteristics, as a result of the numerical solution of the lubricant flow and heat transfer, are used to search for the optimal pa- rameters of a thrust bearing. Each solution (marked as an individual) is represented by a set of variables (marked as genes) and is evaluated us- ing integral characteristics (marked as the objective function). To create a new generation, the fitness function is calculated for each individual, based on the objective function. The algorithm thus searches for the global minimum of the objective function, depending on the genes. In this case, the fitness function is expressed as a negative value of the objective function and expresses the quality of the thrust bearing design represented by the individual. Individuals are stochastically selected and modified by the genetic operators, including a selection, a crossover and a mutation.

After the application of these genetic operators, a new generation is created. The proposed strategy includes a generation model of GA constrained by the limit values of genes and elitism. In this model, a new generation of individuals is created with each iteration, while a predetermined pro- portion of the best individuals (referred to as elite individuals) from the previous generation is maintained [18]."

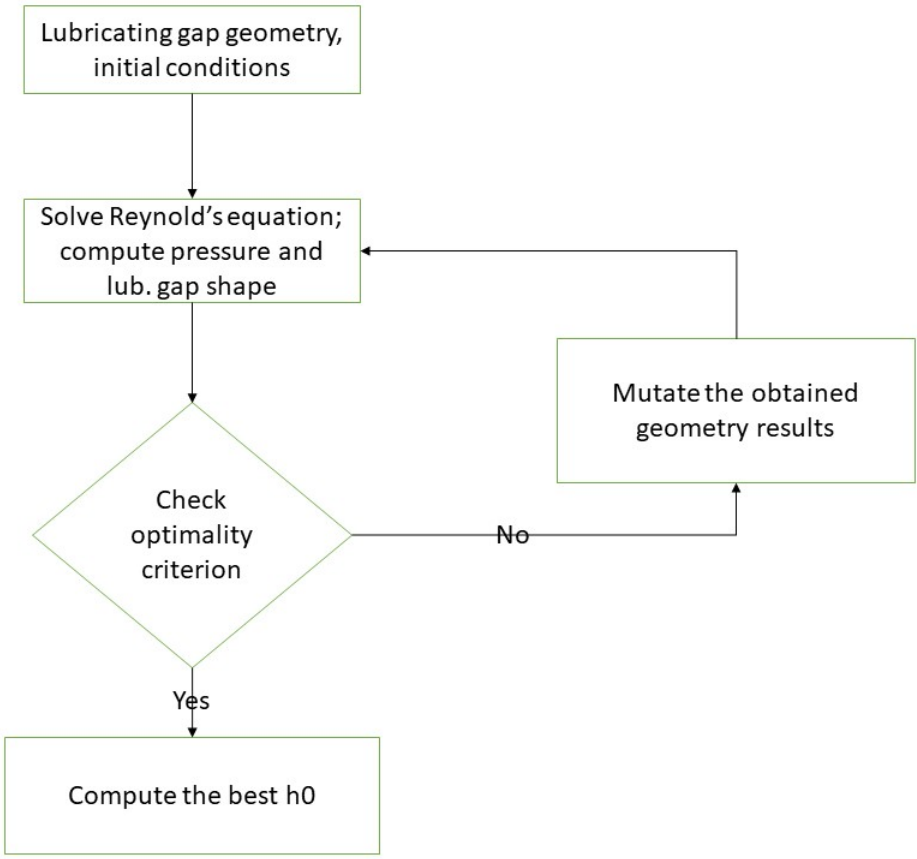

Figure 15: Flowchart for Adapted Genetic Algorithm

4 Results and Discussions

4.1 Initial Problem

Minimum Lubricating Gap, h_0

Applying the Newton-Raphson method, section (3.3), is an initial guess of 0.0005 is taken. Adequate care was taken to make sure that we do not go below the recommended minimum gap thickness of 3 micrometers.

The problem of initial geometry for the lubrication gap was using Newton's Method in MATLAB. The codes can be found in the Appendix section.

The Jacobian can be applied to assist the Newton's method. Some of the downsides of the Newtons method can be glossed over with the Jacobian method.[13]

Applying Jacobian to Newtons Method

Finding the derivative terms:

$$x_{n+1} = x_n - \frac{f(x_n)}{f'(x_n)}$$

From the above figure, it is apparent that:

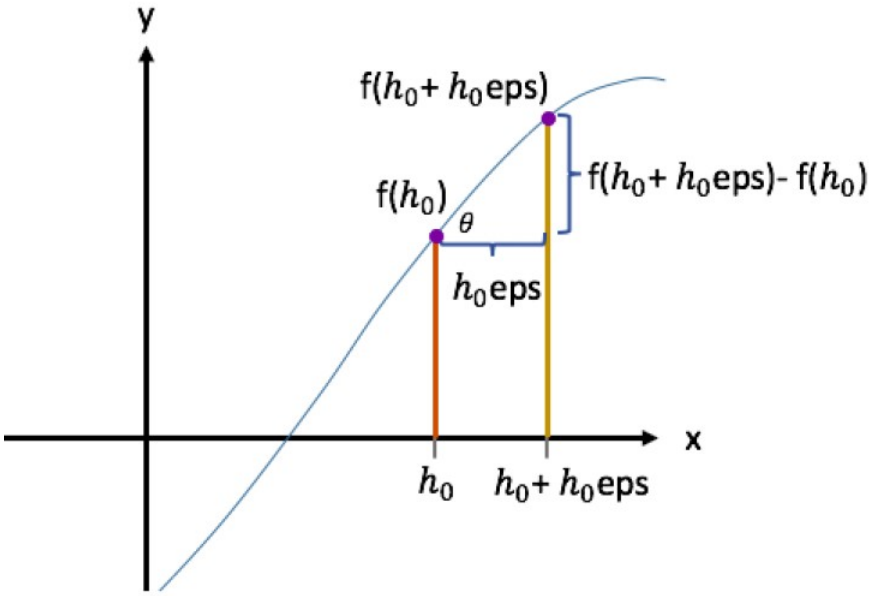

Figure 16: Newton Method with Jacobian
[13]

$$\tan\theta = \frac{f\left(h_0 + h_0 eps\right) - f\left(h_0\right)}{h_0 eps} \tag{4.1}$$

The result was obtained thus:

1. It starts off with the initial guess of $h_0 = 0.0005$. The convergence ratio K is then computed with this initial h_0

2. With the given load, W, and h_0, we compute the difference $f = f(h_0) - W$.

3. The change in x, $\triangle x$ is $h_0 epps$. With this value, we recompute the difference $ff = f(h_0 + eps) - W$

4. Equate the jacobian to $(ff - f)/h_0 eps$; this coincides with tanθ in the figure above.

5. For the next iteration of h_0 is computed by $h_0 = h_0 - 0.0009.f/jacobian$

6. Comparing the two values f and W, we take a ratio of both of them. To adjust for errors, we repeat the calculation until the error is less than 1e-4, i.e. the approximation point is closed or almost equal to the root answer [13].

The initial geometry for the problem was obtained to be 0.0004695 m $\approx$ 0.45mm.

4.1.1 Analytical Results

The analytical results are computed using the equations from section(3.4.2)

Load Capacity:

$$\frac{\mathbf{W}}{\mathbf{L}} = \frac{\mathbf{6U\eta B^2}}{\mathbf{K^2 {h_0}^2}} \left(-\ln(\mathbf{K+1}) + \frac{\mathbf{2K}}{\mathbf{K+2}} \right) \tag{4.2}$$

Friction force:

$$\frac{\mathbf{F}}{\mathbf{L}} = \frac{\mathbf{U\eta B}}{\mathbf{h_0}} \left(\frac{6}{\mathbf{K+2}} - \frac{4\ln(\mathbf{K+1})}{\mathbf{K}} \right) \tag{4.3}$$

Coefficient of friction:

$$\mu = F/W \tag{4.4}$$

Lubricant flow rate:

$$\frac{Q_{\mathrm{J}}}{\mathrm{L}} = \mathrm{Uh_0} \left(\frac{\mathbf{K+1}}{\mathbf{K+2}} \right) \tag{4.5}$$

The analytical results were for the initial problem were computed for different values of K, the convergence ratio.

The maximum load capacity occurs at K = 1.2 but the minimum coefficient of friction is obtained when K = 1.55.[12]

Table 1: Analytical Results

Quantity	K = 1.55	K = 1.2
W	1.0077 kN	1.0288 kN
F	46.4385 N	48.2054 N
Q	$0.0215 m^3/s$	$0.0206 m^3/s$

4.1.2 Numerical Results

Non-dimensional Reynolds equation

The non-dimensional Reynolds Equation:

$$\frac{\partial}{\partial \bar{x}} \left(\bar{\mathrm{h}}^3 \frac{\partial \bar{p}}{\partial \bar{x}} \right) + \frac{R^2}{L^2} \frac{\partial}{\partial \bar{z}} \left(\bar{\mathrm{h}}^3 \frac{\partial \bar{p}}{\partial \bar{z}} \right) = \frac{\partial \bar{h}}{\partial \bar{x}} \tag{4.6}$$

where:

- $$\bar{h} = h/C \tag{4.7}$$
- the clearance:

$$C = (h_{max} + h_{min})/2 \tag{4.8}$$

- the relationship between the pressure and the non-dimensional pressure is given by:

$$p = 6U\eta\frac{R}{C^2}\bar{p} \tag{4.9}$$

- The length of the bearing pad, L:

$$L = R_1 - R_0 \tag{4.10}$$

- R is the mean bearing radius.

Using the finite difference method, the terms of the equation are:

$$\left(\bar{\mathrm{h}}^{-3}\frac{\partial\bar{p}}{\partial\bar{x}}\right) = \frac{\bar{h}^3_{i+0.5,j}\cdot\bar{p}_{i+1,j} + \bar{h}^3_{i-0.5,j}\bar{p}_{i-1,j} - \left(\bar{h}^3_{i+0.5,j} + \bar{h}^3_{i-0.5,j}\right)\cdot\bar{p}_{i,j}}{(\Delta\bar{x})^2} \tag{4.11}$$

$$\left(\bar{\mathrm{h}}^{-3}\frac{\partial\bar{p}}{\partial\bar{z}}\right) = \frac{\bar{h}^3_{i,j+05}\cdot\bar{p}_{i,j+1} + \bar{h}^3_{i,j-0.5}\bar{p}_{i,j-1} - \left(\bar{h}^3_{i,j+0.5} + \bar{h}^3_{i,j-0.5}\right)\cdot\bar{p}_{i,j}}{(\Delta\bar{z})^2} \tag{4.12}$$

$$\frac{\partial\bar{h}}{\partial\bar{x}} = \frac{\bar{h}_{t+1,j} - \bar{h}_{t-1,j}}{2\Delta\bar{x}} \tag{4.13}$$

The nondimensional Reynolds equation is re-written as:

$$\begin{aligned}\left(\bar{h}^3_{i+0.5,j}\cdot\bar{p}_{i+1,j} + \bar{h}^3_{i-0.5,j}\bar{p}_{i-1,j} - \left(\bar{h}^3_{i+0.5,j} + \bar{h}^3_{i-0.5,j}\right)\bar{p}_{i,j}\right) + \frac{R^2}{L^2}\left(\frac{\Delta\bar{x}}{\Delta\bar{z}}\right)^2\bar{h}^3_{i,j}\left(\bar{p}_{i,j+1} + \bar{p}_{i,j-1} - 2\cdot\bar{p}_{i,j}\right)\\ = \frac{\Delta\bar{x}}{2}\left(\bar{h}_{i+1,j} - \bar{h}_{i-1,j}\right)\end{aligned} \tag{4.14}$$

$$\begin{aligned}\left(\bar{h}^3_{i+0.5,j}\cdot\bar{p}_{i+1,j} + \bar{h}^3_{i-0.5,j}\bar{p}_{i-1,j}\right) + \frac{R^2}{L^2}\left(\frac{\Delta\bar{x}}{\Delta\bar{z}}\right)^2\bar{h}^3_{i,j}\left(\bar{p}_{i,j+1} + \bar{p}_{i,j-1}\right) - \frac{\Delta\bar{x}}{2}\left(\bar{h}_{i+1,j} - \bar{h}_{i-1,j}\right)\\ = \left(\bar{h}^3_{i+0.5,j} + \bar{h}^3_{i-0.5,j} + \frac{2R^2}{L^2}\left(\frac{\Delta\bar{x}}{\Delta\bar{z}}\right)^2\bar{h}^3_{i,j}\right)\cdot\bar{p}_{i,j}\end{aligned} \tag{4.15}$$

Pressure Distribution

Using the non-dimensional parameters, the non-dimensional pressure distribution that solves the Reynolds equation for this setup (system) was computed. The numerical version of the Reynolds equation, was computed using Finite Difference Method.[19]

The nodal non-dimensional pressure is then:

$$\bar{p}_{i,j} = \left(\frac{\bar{h}^3_{i+0.5,j}}{\left(\bar{h}^3_{i+0.5,j} + \bar{h}^3_{i-0.5,j} + \frac{2R^2}{L^2}\left(\frac{\Delta\bar{x}}{\Delta\bar{z}}\right)^2\bar{h}^3_{i,j}\right)}\cdot\bar{p}_{i+1,j} + \frac{\bar{h}^3_{i-0.5,j}}{\left(\bar{h}^3_{i+0.5,j} + \bar{h}^3_{i-05,j} + \frac{2R^2}{L^2}\left(\frac{\Delta\bar{x}}{\Delta\bar{z}}\right)^2\bar{h}^3_{i,j}\right)}\bar{p}_{i-1,j}\right) +$$

$$+\frac{\frac{R^2}{L^2}\left(\frac{\Delta\bar{x}}{\Delta\bar{z}}\right)^2\bar{h}_{i,j}^3}{\left(\bar{h}_{i+0.5,j}^3+\bar{h}_{i-05,j}^3+\frac{2R^2}{L^2}\left(\frac{\Delta\bar{x}}{\Delta\bar{z}}\right)^2\bar{h}_{i,j}^3\right)}\cdot(\bar{p}_{i,j+1}+\bar{p}_{i,j-1})-\frac{\Delta\bar{x}}{2}\frac{\left(\bar{h}_{i+1,j}-\bar{h}_{i-1,j}\right)}{(\bar{h}_{i+0.5,j}^3+\bar{h}_{i-0.5,j}^3+\frac{2R^2}{L^2}\left(\frac{\Delta\bar{x}}{\Delta\bar{z}}\right)^2\bar{h}_{i,j}^3\right)} \tag{4.16}$$

The mesh used is a square mesh:

$$\frac{\Delta\bar{x}}{\Delta\bar{z}}=1 \tag{4.17}$$

Making this substitution, and removing the j subscript from the h terms, we obtain:

$$\begin{aligned}\bar{p}_{i,j}=&\left(\frac{\bar{h}_{i+0.5}^3}{\left(\bar{h}_{i+0.5}^3+\bar{h}_{i-0.5}^3+\frac{2R^2}{L^2}\bar{h}_i^3\right)}\cdot\bar{p}_{i+1,j}+\frac{\bar{h}_{i-0.5}^3}{\left(\bar{h}_{i+0.5}^3+\bar{h}_{i-05}^3+\frac{2R^2}{L^2}\bar{h}_i^3\right)}\bar{p}_{i-1}\right)+\\&+\frac{\frac{R^2}{L^2}\bar{h}_i^3}{\left(\bar{h}_{i+0.5}^3+\bar{h}_{i-05}^3+\frac{2R^2}{L^2}\bar{h}_i^3\right)}\cdot(\bar{p}_{i,j+1}+\bar{p}_{i,j-1})-\frac{\Delta\bar{x}}{2}\frac{\left(\bar{h}_{i+1}-\bar{h}_{i-1}\right)}{(\bar{h}_{i+0.5}^3+\bar{h}_{i-0.5}^3+\frac{2R^2}{L^2}\bar{h}_i^3)}\end{aligned} \tag{4.18}$$

which is written compactly as:

$$\bar{p}_{i,j}=A_i\cdot\bar{p}_{i,j+1}+B_i\cdot\bar{p}_{i,j-1}+C_i\cdot\bar{p}_{i+1,j}+D_i\cdot\bar{p}_{i-1,j}+E_i \tag{4.19}$$

Load Capacity

$$W=\sum_0^B P_{i,j}\Delta x \tag{4.20}$$

Friction Force

$$F=\sum_0^B\frac{(P_{i+1,j}-P_{i-1,j})\Delta x}{2\Delta x}\frac{h}{2}+\frac{\eta U}{h} \tag{4.21}$$

Coefficient of friction

$$\mu=\frac{F}{W} \tag{4.22}$$

Lubricant flow rate

$$\dot{m}=-\sum_0^B\Delta z(\frac{-h^3}{12\eta}\frac{(P_{i+1,j}-P_{i-1,j})}{2\Delta x}+\frac{Uh}{2}) \tag{4.23}$$

Numerical Results

Solving the non-dimensional Reynolds equation numerically, the following results were obtained:

Table 2: Numerical Results

Quantity	Value
p_{max}	55.39 kPa
W	1.1078 kN
F	45.7231 N
Q	$0.0084 m^3/s$

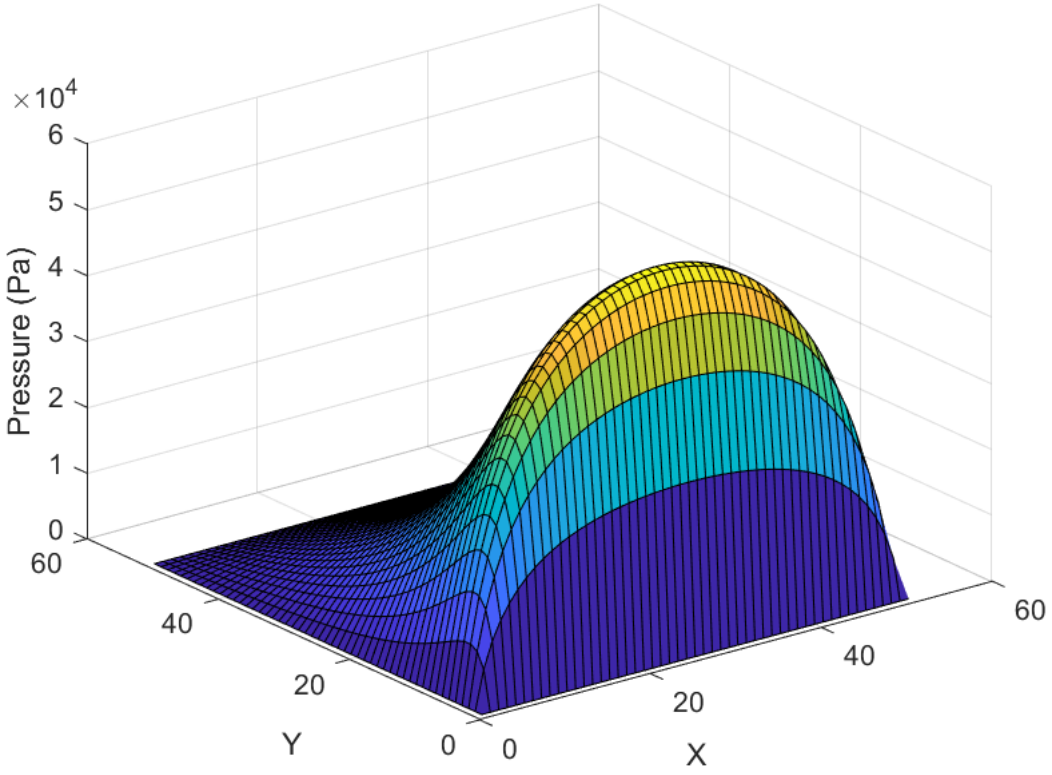

Figure 17: Pressure Profile for Initial Problem

4.2 General Gap Profile

The non-dimensional Reynolds equation was solved numerically for the described General Gap Profile shown in section (3.4.3).

For simplicity, the general profile was chosen by discretizing a variation of the analytical profile described by equation (3.51); five control points were introduced.

$$h = h_0 \left(1 + \frac{h_1 - h_0}{h_0} \frac{x}{B}\right) \tag{4.24}$$

The general gap profile shape can be varied by changing any of its five control points.

These control points are a ratio of an arbitrary gap size to the initial lubricating gap:

$$H(i) = \frac{h(i)}{h_0} \tag{4.25}$$

For this generalized profile, these five control points were used:
The following results were obtained:

Table 3: Control points for General Profile

x	0.00	0.25	0.50	0.75	1.00
H	7.1602	13.967	20.7737	27.5804	34.3871

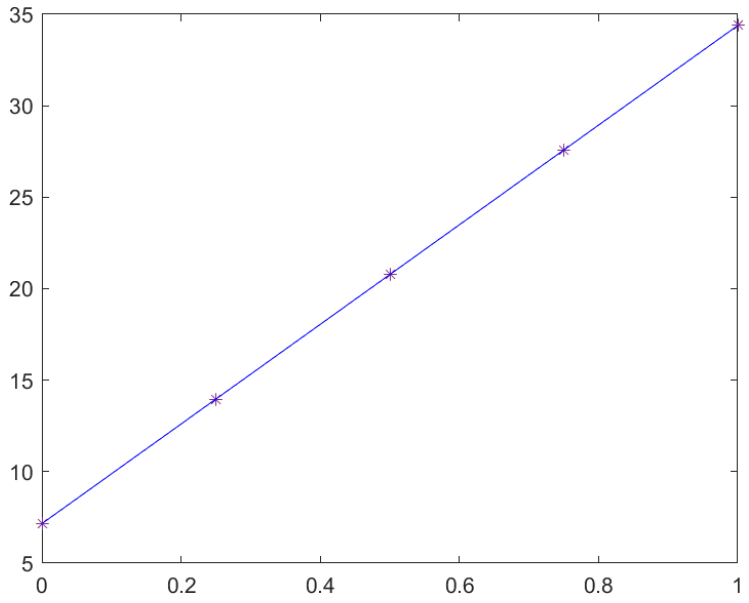

Figure 18: General Profile

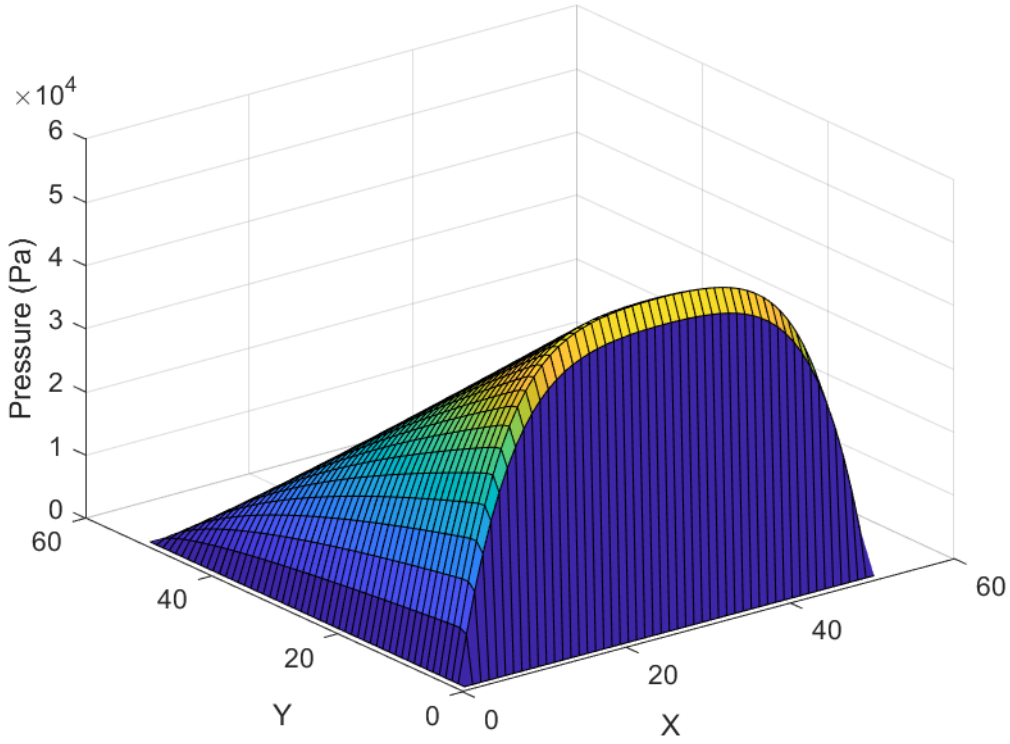

Figure 19: Pressure Profile for General Profile

4.3 Scalarization of Objective function

Considering that the problem is a multiobjective function, the objective function to be minimized is given as:

Table 4: General Gap Profile Results

Quantity	Value
p_{max}	51.727 kPa
W	1.0345 kN
F	46.384 N
Q	$0.0023m^3/s$

$$f_{\text{obj}}(\mathbf{x}) = \frac{\sum_{k=1}^{\max} f_{\text{f},k} s_{\text{m},k} s_{\text{w},k} w_k}{\sum_{k=1}^{k_{\max}} w_k} \tag{4.26}$$

Where k reflects the number of operating conditions, in this case, the various control points, the initial bearing design x_{init} is the initial parent vector and w_k is the weighting factor selected depending on the operating conditions of the bearing. [18]

The problem is considered under one operating condition, hence, k= 1.

Given that the effect of friction is to be reduced, the load capacity of the bearing exceeds the minimum requirement of 1000 N and that the requirement of the lubricant flow rate is that it is not increased. The first, and most important objective (as mentioned in section), is the friction force

The friction torque ratio (f_f) is proposed relative to the friction torque of the initial bearing design($M_{f,init}$) under the considered operating condition of the form:

$$f_{\text{f}} = \frac{M_{\text{f}}}{M_{\text{f,init}}} \tag{4.27}$$

The lubricant flow rate factor increases the value of the objective function in this case where we have an upper-limit to the increase of lubricant flow rate; "Do not increase lubricant flow rate."

$$s_{\text{m}} = \max\left(1, \left(\frac{\dot{m}_{\text{r}}}{\beta_m \dot{m}_{\text{r,init}}}\right)^{\lambda}\right) \tag{4.28}$$

where $\beta_m \geq 1$. The factor $\beta_m = 2$ was chosen. This factor increases the tolerable lubricant flow rate and $\lambda \geq 1$ is a power exponent In his work, Novotný et al [18] suggests that a reasonable number for $\lambda = 3$.

After being unable to find in searched literature, the load capacity factor was created uniquely to satisfy the requirement of the thesis problem. It is defined as follows:

$$s_{\text{w}} = \left(\frac{1}{\min\left(1, \left(\frac{W_{\text{i}}}{W_{\text{init}}}\right)^{\lambda}\right)}\right) \tag{4.29}$$

4.4 GA Results

In the setup of the multiobjective optimization problem, the variables consist of the five control points defining the general profile. Hence, the set of optimal solutions is made of the limit points of each of the control points of the general gap profile.

$$\begin{aligned} h_1 &\in [3 * 10^{-6}, 0.047]m \\ h_2 &\in [3 * 10^{-6}, 0.047]m \\ h_3 &\in [3 * 10^{-6}, 0.047]m \\ h_4 &\in [3 * 10^{-6}, 0.047]m \\ h_5 &\in [3 * 10^{-6}, 0.047]m \end{aligned} \tag{4.30}$$

The scalarized objective function was then fed as input to the GA. After may iterations, the GA stochastically found an optimal profile.

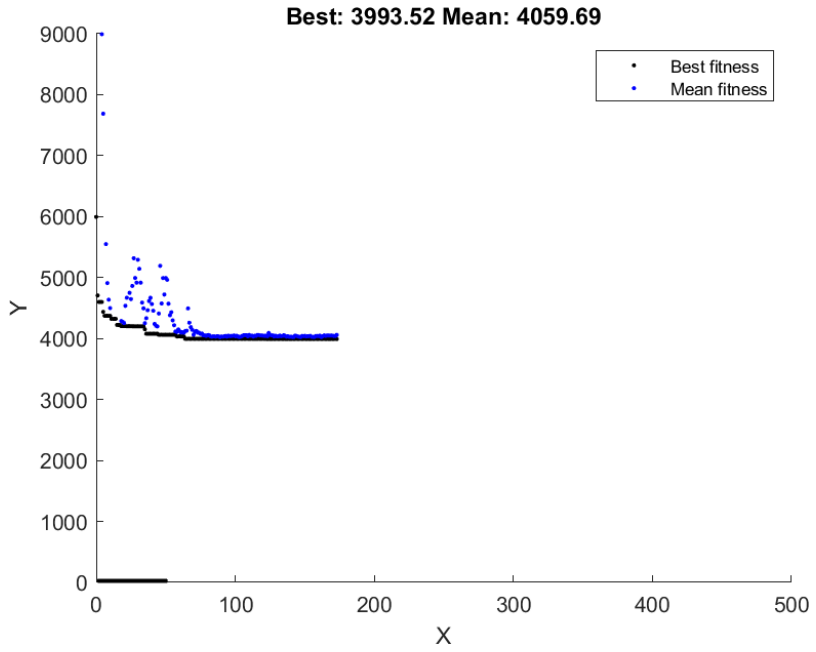

Figure 20:

4.5 Optimal Gap Profile

The GA yielded the following optimal lubricating gap profile:

Table 5: GA Generated Profile

x	0.00	0.25	0.50	0.75	1.00
H	49.289	55.3842	62.4315	89.6601	95.3201

The results of the optimal profile:

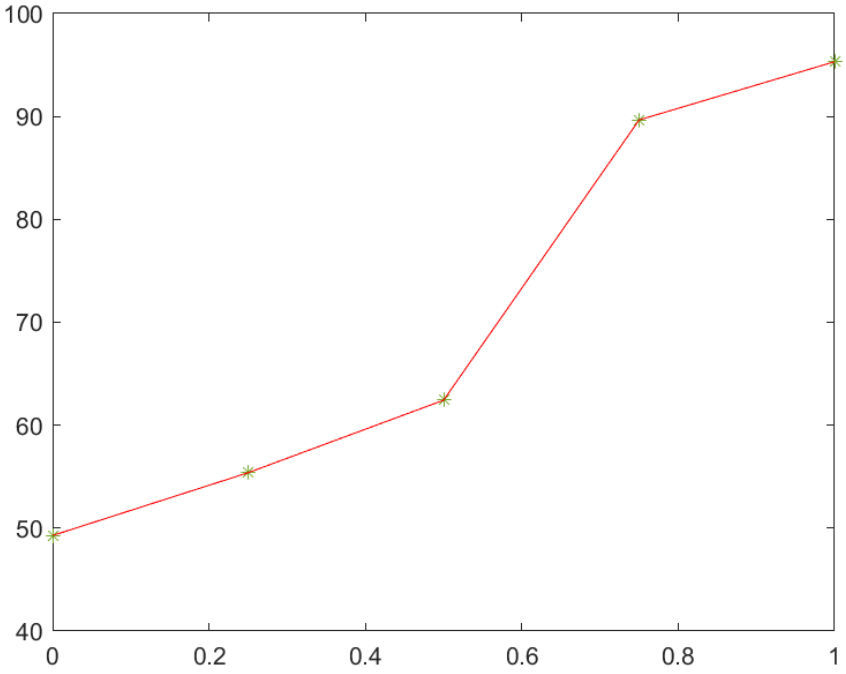

Figure 21: Optimal Profile

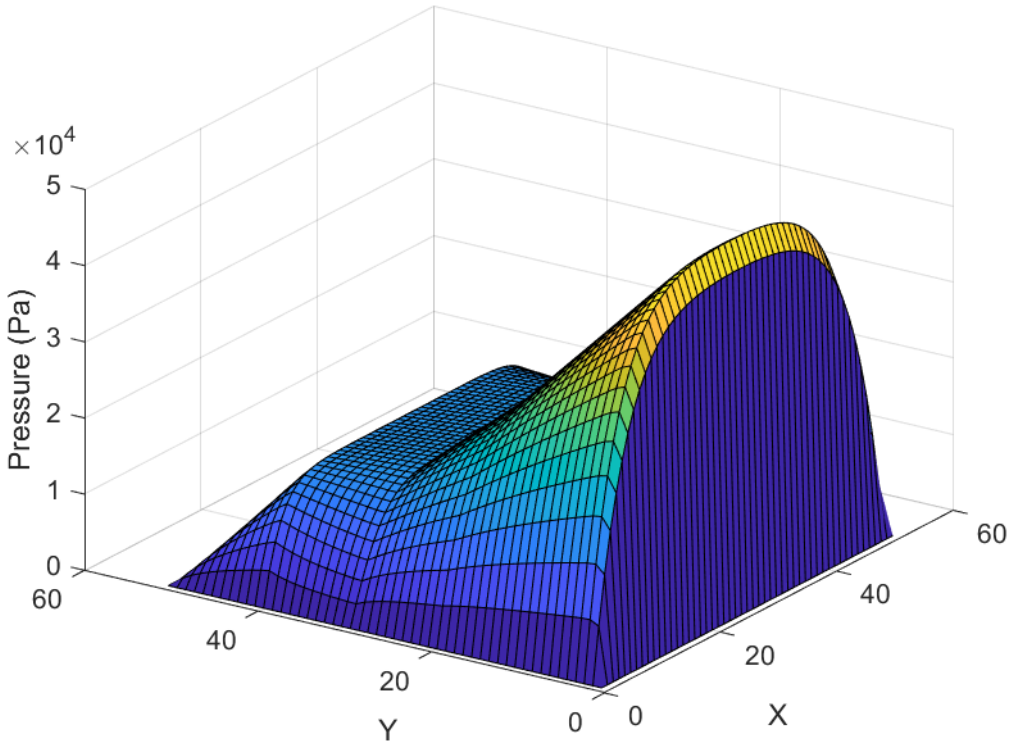

Figure 22: Pressure Profile for Optimal Profile

4.6 Discussion

4.6.1 Analytical and General Gap Profile Results

Comparing the Analytical Results against the General Profile Results, the following results were obtained:

Table 6: Optimal Profile Results

Quantity	Value
p_{max}	4.922 kPa
W	963.7373 N
F	45.79 N
Q	$0.0024m^3/s$

Table 7: Comparison of Analytical and General Profile Results

Quantity	K = 1.55	K = 1.2	General Profile
W	1.0077 kN	1.0288 kN	1.0345 kN
F	46.4385 N	48.2054 N	46.8398 N
Q	$0.0215m^3/s$	$0.0206m^3/s$	$0.0023m^3/s$

The general gap profile has:

- a sufficient load capacity that satisfies the 1000 N minimum requirement.
- the lubricant flow rate is not increased.
- near-equivalent friction force as that of the analytical profile for the specified problem.

4.6.2 Analytical and Optimized Profile Results

Comparing the Analytical Results against the Optimized Profile Results, the following results were obtained:

Table 8: Comparison of Analytical and Optimized Profile Results

Quantity	K = 1.55	K = 1.2	Optimized Profile
W	1.0077 kN	1.0288 kN	963.7373 N
F	46.4385 N	48.2054 N	45.79 N
Q	$0.0215m^3/s$	$0.0206m^3/s$	$0.0018m^3/s$

From this result, note that:

- The load capacity for the optimized profile is close to the required 1000 N.
- The size of lubricating gap (of the control points) is from the set of feasible solutions in equation(4.30).
- The lubricant flow rate is not increased in the optimized profile.
- The "most important" objective function, the friction force of the setup, is reduced in the optimized profile.

5 Conclusion

5.1 Parameter Choice

The chosen parameter should be one that affects the integral parameters to be considered by the study. The lubricating gap size affects the mechanical efficiency of the thrust bearing, and turbocharger. The shape and size of the lubricating gap determines the amount of pressure that can be developed by the setup. The pressure affects the load capacity, friction force, and the lubricant flow rate. These are integral parameters of a thrust bearing being considered.

The choice of parameter is sufficient for the integral parameters of the thrust bearing being considered.

5.2 Genetic Algorithm: Strengths and Weaknesses

As stated in Section 3.5.1, the Genetic Algorithm has its strengths and weaknesses.

5.2.1 Strengths

- It is useful in finding global solution of multi-objective function. The thesis problem is a case in point. The GA was able to find a solution for the multi-objective function.
- It effortlessly captures multiple non-inferior solutions.
- It uses probabilistic and not deterministic operators. It moves randomly from one solution to another; not following a defined path to finding a solution.
- It is less likely to be trapped in a local minimum. While running the GA for the problem, if the codes are not seeded to return a previously provided solution, the result for each attempt might differ from the next.
- Provides local and global solution.
- In many cases, they are less sensitive to the presence of noise and uncertainty in measurements.

5.2.2 Weaknesses

- It requires comparatively less information about the problem. To formulate the objective function, a product of factors was computed. This product of factors was the objective function inputed into the GA. This product was a number. The GA optimized this problem with upper and lower limits to the lubricating gap size. This is too little information to describe the working condition of the turbocharger.
- It is computationally time consuming. A single solution of a bearing steady state may include hours of computational time on high-performance computers. This fact makes it practically impossible to use these calculations for multiple repetitive tasks

involving the solution of hundreds or thousands of operating states.

- Despite the fact that GA for the thesis problem was relatively simple, coding the equations the equations to generate the required factors for the multiobjective function is time consuming.

5.2.3 Measures Taken to Mitigate Weaknesses

- The MATLAB code that solves the Reynolds equation, for a general profile, was embedded in the objective function. With this, a little more is done to input more information about the problem into the GA.

- To reduce computational time, the MATLAB code that solves the Reynolds equation was optimized to compute the solution to the problem in less than a minute (0.3906s).

5.3 Working Profile Description

The general profile was described and optimized using suitable means.

The integral parameters of the optimal profile, compared with the analytical description of the working profile, has :

- Near-sufficient load capacity.

- Lower friction.

The optimal profile also followed the listed directives for the optimization problem:

- Does not increase lubricant flow rate.

- The minimum lubrication gap size was not exceeded.

5.4 Why is the working profile better?

The general profile allows for flexibility of the design of the thrust bearing.

When compared to the analytical description of the working profile, it better models the working conditions of the thrust bearing. With the control points, the shape of the lubricating gap profile can be altered.

The existing series-used bearing, analytical description of the working profile, uses elemental shapes; it makes solving for integral parameters easier, but does not consider realistic working conditions of the thrust bearing. The thrust bearing lubricating gap

profile, while working, takes up more shapes than can be described by elementary shapes.

Given that less friction losses are incurred from the optimized results of the general profile, the design of the working surfaces of the thrust bearing using optimized general profiles would provide better results with respect to integral parameters.

5.5 Application of Study

The results from this study can be applied to:

- Modeling for study of the working profile of the thrust bearing
- Designing more realistic and robust lubricating gap profiles for thrust bearings of turbochargers.
- Optimizing general lubricating gap profiles described by other means besides the one used in the study.

5.6 Future Work

The results of this thesis are, in this state, not applicable in industry.

Some suggestions to improve the applicability of the results:

1. The profile Fig.18 was described by a piecewise linear function. The resulting optimized profile Fig. 21 can be seen to be piecewise linear. Description of the working profile by a smoother function could make results easily applicable in industry.
2. For the thesis problem, five (5) control points were used to discretize the working profile. If more control points are used in the study of this problem, finer and applicable profiles could be obtained.

6 References

References

[1] EPI. Inc. (2017, May 5). *Turbochargers*. http://http://www.epi-eng.com/piston_engine_technology/turbocharger_technology.htm

[2] Charitopoulos A.G, Visser R., Eling R., Papadopoulos C.I .(2018) *Design Optimization of an Automotive Turbocharger Thrust Bearing Using a CFD-Based THD Computational Approach. Lubricants*. 2018; 6(1):21. https://doi.org/10.3390/lubricants6010021

[3] NGUYEN-SCHÄFER, H. (2015). Rotordynamics of Automotive Turbochargers. (2nd edition). Ludwigsburg, Germany: Springer. ISBN 978-3-319-17643-7.

[4] Wasilczuk, M. (2015). *Friction and Lubrication of Large Tilting-Pad Thrust Bearings*. Lubricants, 3(2), 164–180. doi:10.3390/lubricants3020164

[5] Wasilczuk, M. (2006, April 12). *Comparison of an optimum-profile hydrodynamic thrust bearing with a typical tilting-pad thrust bearing*. Lubrication Science. https://doi.org/10.1002/ls.3010150306

[6] Yu, H., Wang, X., Zhou, F.(2010) *Geometric Shape Effects of Surface Texture on the Generation of Hydrodynamic Pressure Between Conformal Contacting Surfaces*. Tribol Lett 37, 123–130 (2010). https://doi.org/10.1007/s11249-009-9497-4.

[7] Gropper, D., Wang, L., Harvey, T.J. (2016) *Hydrodynamic lubrication of textured surfaces: A review of modeling techniques and key findings*. Tribology International, Volume 94, 2016, Pages 509-529, ISSN 0301-679X, https://doi.org/10.1016/j.triboint.2015.10.009.

[8] Hashimoto, H. (1998). *Optimization of Oil Flow Rate and Oil Film Temperature Rise in High Speed Hydrodynamic Journal Bearings*. Tribology and Interface Engineering Series, 34, 205-210.

[9] LUKE, S. (2013) Essentials of Metaheuristics. (2nd edition). ISBN 9781300549628.

[10] Bullock, G. N., Denham, M. J., Parmee, I. C., Wade, J. G. (1995). *Developments in the use of the genetic algorithm in engineering design*. Design Studies, 16(4), 507–524. https://doi.org/10.1016/0142-694x(95)00023-k

[11] Avraham, H. (2002). Bearing Design in Machinery: Engineering Tribology and Lubrication. New York: Marcel Dekker.

[12] STACHOWIAK Gwidon W. and BATCHELOR Andrew W. (2005) Engineering Tribology.(4th edition) Butterworth-Heinemann. ISBN 0-7506-7836-4.

[13] Sawadkosin, P., (2019). *Shape Optimization of Machine Components due to Variability of Input Data*, Institute of Mathematics, Brno University of Technology.

[14] WAZIRI M.Y., LEONG W.J., HASSAN M.A., MONSI M. Jacobian (2010). *Computation-Free Newton Method for Systems of Non-Linear Equations*. Journal of numerical Mathematics and stochastic, 2(1):5463, 2010.

[15] Sokolowski, J., Zolesio, J.P., (1992). Introduction to Shape Optimization : Shape Sensitivity Analysis, Springer-Verlag Berlin Heidelberg, New York.

[16] Nyoman, G. (2018). *A review of multi-objective optimization: Methods and its applications*. Cogent Engineering, 5:1, 1502242. doi: 10.1080/23311916.2018.1502242.

[17] Ulivieri, V (2014). *Multicriteria Optimization: Scalarization techniques*. Sant'Ama School of Advanced Studies, Department of Economics and Management. University of Pisa.

[18] Novotný, P., Jonák, M., Vacula, J., (2021). *Evolutionary Optimisation of the Thrust Bearing Considering Multiple Operating Conditions in Turbomachinery*. International Journal of Mechanical Sciences, Volume 195, 2021, 106240, ISSN 0020-7403, https://doi.org/10.1016/j.ijmecsci.2020.106240.

[19] Hirani, H. (2012, November 12). *Finite Difference Method to Solve Reynolds Equation*. https://www.youtube.com/watch?v=Um1wxAHMmjo&t=1s

List of Figures

1 Borg-Warner Turbocharger with Variable Geometry Turbine 12
2 Schematic of Hydrodynamic Bearing 13
3 Initial Problem 15
4 Equilibrium of an element of fluid from a hydrodynamic film 22
5 Velocity profiles at the entry of the hydrodynamic film. 25
6 Continuity of flow in a column 25
7 Unidirectional Approximation 27
8 Pressure distribution in the long bearing approximation 29
9 Pressure distribution for Linear Pad bearing 29
10 Load components acting on a hydrodynamic bearing. 31
11 Newton-Raphson Method 32
12 Example of a pad bearing application to sustain the thrust loads from the ship propeller shaft. 33
13 Geometry of a linear pad bearing. 34
14 Flowchart for Genetic Algorithm 46
15 Flowchart for Adapted Genetic Algorithm 48
16 Newton Method with Jacobian 49
17 Pressure Profile for Initial Problem 53
18 General Profile 54
19 Pressure Profile for General Profile 54
20 GA Result 56
21 Optimal Profile 57
22 Pressure Profile for Optimal Profile 57

List of Tables

1 Analytical Results 50
2 Numerical Results 53
3 Control points for General Profile 54
4 General Gap Profile Results 55
5 GA Generated Profile 56
6 Optimal Profile Results 58
7 Comparison of Analytical and General Profile Results 58
8 Comparison of Analytical and Optimized Profile Results 58

7 APPENDIX

(FIND H0)

```
function h0 = GETH0byNewton
h0eps = 1e-8;
errF = 0.0001;
err = 1;
frad = 100; % loading
rpm = 45000;
m = 6;
alpha = 0.5;
R0 = 0.030;
R1 = 0.060;
rpmtomms = rpm *2* pi *(R0+R1) /(2*60) ;
B = pi *(R0+R1)/m;
L = R1 - R0;
eta = 0.01; % constant viscosity
h0 = 0.0005;
while err > errF
    k = B*tand(alpha) /h0;
    fu = -(6* eta* rpmtomms *L*B ^2) *(-log(k +1) +(2* k)/(k +2) )/(( k ^2) *(h0 ^2) )
    f = fu - frad ;
    h0 = h0+ h0eps ;
    kk = B* tan(alpha *pi /180) /h0;
    fu = -(6* eta* rpmtomms *L*B ^2) *(-log(kk +1) +(2* kk)/(kk+2) ) /((kk ^2) *(h0 ^
    f1 = fu - frad ;
    h0 = h0 - h0eps ;
    jacobian = (f1 -f)/ h0eps ;
    h0 = h0 - 0.0009* f/ jacobian ;
    err = abs (f/ frad );
end
end
```

```
    (NUMERICAL SOLUTION)

function [Pmax, Load_init, Fric_init, mu, Mf_init] = NumSolReyEqn(R0, R1, N, alpha, rh
%% INPUT DATA

eta = 0.01;
R = (R1+R0)/2;
U = N/60 * 2*pi *R;
rho = 840;
h0 = 4.695e-4;


M = 50;
N = 50;
X1 = 0.045;% Maximum distance in x-direction in m



L = R1-R0;
K = 0.2788;
B = 0.0471;



Z1 =  0.045; % Maximum distance in z-direction in m
hmin = h0+ 10e-3* tand(alpha);
hmax = h0 + 15e-3*tand(alpha);
C = (hmax + hmin)/2;
delxbar = 1/N;
delzbar = 1/M;
% the nondimensional parameter x-sq/z-sq
const1 = X1*X1/(Z1*Z1);
ITER = 1000;

%% initizialization of the pressure
for i=1:N+1
    for j=1:M+1
        p(i,j)= 0.0;
        Press(i,j) = 0.0;
    end
end
sum(1) = 0.0;

%% second iteration
for k = 1:ITER
    sumij = 0.0;
    for i = 2:N
        % it is know the initial and final pressure
```

```
        % it is the ambient pressure which equals zero
        % this loop incorporates the boundary condition
        x(i) = 1/N * (i-1);

        % film thickness
        % consider using the description it was given in the specific
        % problem

            h = h0/C * (1 + K*x(i)/B);
            hm = h0/C * (1 + K*(x(i)-0.5*delxbar)/B); % h at half node(left)
            hp = h0/C * (1 + K*(x(i)+0.5*delxbar)/B); % h at half node(right)
            hm1 = h0/C * (1 + K*(x(i)-delxbar)/B); % h at one node (left)
            hp1 = h0/C * (1 + K*(x(i)+delxbar)/B); % h at one node (right)

        % cubic terms
        cubh = h*h*h;
        cubhm = hm*hm*hm;
        cubhp =hp*hp*hp;
        const2 = (cubhp+cubhm+2*const1*cubh);
        A = const1 * cubh/const2;
        CA = cubhp/const2; % constant C
        D = cubhm/const2;
        E = 0.5*delxbar*(hp1-hm1)/(const2);

        for j=2:M
            Z(j)=1/M *(j-1);
            p(i,j) = A*p(i,j+1)+A*p(i,j-1)+CA*p(i+1,j)+D*p(i-1,j) + E;
            Press(i,j) = p(i,j) .* (U * 6 * R * eta /C^2);
            sumij = sumij + p(i,j);
        end
    end

    sum(k+1) = sumij;

    % for our convergence criterion
    percentage = abs(sum(k+1) -sum(k))/abs(sum(k+1));
    if percentage < 0.00001
        break
    end
end

y = k;
surf(Press);
xlabel('X'); ylabel('Y'); zlabel('Pressure (Pa)');

%% SEARCH FOR MAXIMUM PRESSURE
Pmax = 0;
for i = 2:N-1
```

```
    for j = 2:M-1
        if Press(i,j) > Pmax
            Pmax = Press(i,j);
        end
    end
end

%% Load Capacity
for i = 1: N
    Load(i,j) = 0;
    for j = 1: M
        Load(i,j) =  Press(i,j).* delxbar;
    end
end

Load_init = 0;
for i = 2:N-1
    for j = 2:M-1
        if Load(i,j) > Load_init
            Load_init = Load(i,j);
        end
    end
end

%% Friction force
for i = 2: N
    Friction(i,j) = 0;
    for j = 2: M
         Friction(i,j) = delxbar .*(((Press(i+1,j) - Press(i-1,j))./(2*delxbar) .*(h*(
    end
end

Fric_init = 0;
for i = 2:N-1
    for j = 2:M-1
        if Friction(i,j) > Fric_init
            Fric_init =  Friction(i,j);
        end
    end
end

%% coefficient of friction

mu = Fric_init/Load_init;

%% flow rate
for i = 2: N
    Mdot(i,j) = 0;
```

```
    for j = 2: M
        Mdot(i,j) = delzbar*((Press(i+1,j) - Press(i-1,j)./(2*delxbar))*(-(h*C)^3/(12*
    end
end

Mf_init = 0;
for i = 2:N-1
    for j = 2:M-1
        if Mdot(i,j) > Mf_init
            Mf_init = Mdot(i,j);
        end
    end
end

end
```

```
    (GENERAL PROFILE)

function [Peemax, LoadCap, Fric, mu, Mf] = GenProfReyEqn(H)


%% SOLVING THE REYNOLDS EQUATION
R0 = 0.03; R1 = 0.06; N1 = 45000; eta = 0.01; alpha = 0.5;  rho = 840;
f = [0.0 0.25 0.5 0.75 1.0];
xmin = 0.0314; xmax = 0.0471; K = 1.55;
 h0 = 4.6959e-04;
N = 50; M = 50;
L = (R1-R0); B = 0.0471;
R = (R1+R0)/2;
U = N1/60 * 2*pi *R;

% clearance
C = (max(H) + min(H))* h0/2;

delxbar = 1/N;
delzbar = 1/M;
% the nondimensional parameter x-sq/z-sq
const1 = R*R/(L*L);
ITER = 1000;
% initizialization of the pressure
for i=1:N+1
    for j=1:M+1
        p(i,j)= 0.0;
        Press(i,j) = 0.0;
    end
end
sum(1) = 0.0;

%% for each of the straight lines that make up the shape of the gap profile
% h(x) = m(i)*(x(i+1) - x(i))+ constant (the equation of a line)
% the constant term is given by (h(i)- (m(i)*(x(i+1)-x(i))))

%% With this idea the general profile is subdivided
%each straight curve forms a segment
% this idea is used to compute the h(i) for each of these segments

%% second iteration
for kk = 1:ITER
    sumij = 0.0;
    for i = 2:N
       Rat = h0/C;
     x(i) = 1/N * (i-1);
        % it is know the initial and final pressure
        % it is the ambient pressure which equals zero
```

```
% this loop incorporates the boundary condition
 if   (i >=2) && (i<= 2*N/5)
    b = H(1) ; a= H(2);
    m = (a - b)/B;
    h = Rat*(1 + m*delxbar );
    hm =  Rat*(1 + m*(delxbar- 0.5*delxbar));
    hp = Rat*(1 + m*(delxbar +0.5*delxbar));
    hm1 = Rat*(1 + m*(delxbar-delxbar)); % h at one node (left)
    hp1 = Rat*(1 + m*(delxbar+delxbar)); % h at one node (right)
end

if  (i >= 2*N/5) && (i<= 3*N/5)
    b = H(2) ; a= H(3);
    m = (a - b)/B;
    h = Rat*(1 + m*delxbar);
    hm =  Rat*(1 + m*(delxbar- 0.5*delxbar));
    hp = Rat*(1 + m*(delxbar +0.5*delxbar) );
    hm1 = Rat*(1 + m*(delxbar-delxbar)); % h at one node (left)
    hp1 = Rat*(1 + m*(delxbar+delxbar) ); % h at one node (right)
end

if   (i >=3*N/5) && (i<=4*N/5)
    b = H(3) ; a= H(4);
    m = (a - b)/B;
    h = Rat*(1 + m*delxbar);
    hm =  Rat*(1 + m*(delxbar- 0.5*delxbar));
    hp = Rat*(1 + m*(delxbar +0.5*delxbar));
    hm1 = Rat*(1 + m*(delxbar-delxbar)); % h at one node (left)
    hp1 = Rat*(1 + m*(delxbar+delxbar)); % h at one node (right)
end

if  (i >=4*N/5) && (i<=N)
    b = H(4) ; a= H(5);
    m = (a - b)/B;
    h = Rat*(1 + m*delxbar);
    hm =  Rat*(1 + m*(delxbar- 0.5*delxbar));
    hp = Rat*(1 + m*(delxbar +0.5*delxbar));
    hm1 = Rat*(1 + m*(delxbar-delxbar)); % h at one node (left)
    hp1 = Rat*(1 + m*(delxbar+delxbar)); % h at one node (right)
end

% cubic terms
cubh = h*h*h;
cubhm = hm*hm*hm;
cubhp =hp*hp*hp;
const2 = (cubhp+cubhm+2*const1*cubh);
A = const1 * cubh/const2;
CA = cubhp/const2; % constant C
```

```
        D = cubhm/const2;
        E = 0.5*delxbar*(hp1-hm1)/(const2);

        for j=2:M
            Z(j)=1/M *(j-1);
            p(i,j) = A*p(i,j+1)+A*p(i,j-1)+CA*p(i+1,j)+D*p(i-1,j) + E;
            Press(i,j) = p(i,j) .* (U * 6 * R * eta /C^2);
            sumij = sumij + p(i,j);
        end
    end

    sum(kk+1) = sumij;

    % for our convergence criterion
    percentage = abs(sum(kk+1) -sum(kk))/abs(sum(kk+1));
    if percentage < 0.00001
        break
    end
end

y = kk;
surf(Press);
xlabel('X'); ylabel('Y'); zlabel('Pressure (Pa)');

%% CALCULATIONS

%% SEARCH FOR MAXIMUM PRESSURE
Peemax = 0;
for i = 2:N-1
    for j = 2:M-1
        if Press(i,j) > Peemax
            Peemax = Press(i,j);
        end
    end
end

%% Load Capacity
for i = 1: N
    Load(i,j) = 0;
    for j = 1: M
        Load(i,j) = Press(i,j).* delxbar;
    end
end

LoadCap = 0;
for i = 2:N-1
    for j = 2:M-1
        if Load(i,j) > LoadCap
```

```
            LoadCap = Load(i,j);
        end
    end
end

%% Friction force
for i = 2: N
    Friction(i,j) = 0;
    for j = 2: M
         Friction(i,j) = delxbar .*(((Press(i+1,j) - Press(i-1,j))./(2*delxbar) .*(h*(
    end
end

Fric = 0;
for i = 2:N-1
    for j = 2:M-1
        if Friction(i,j) > Fric
            Fric = Friction(i,j);
        end
    end
end

%% coefficient of friction

mu = Fric/LoadCap;


%% Lub flow rate
for i = 2: N
    Mdot(i,j) = 0;
    for j = 2: M
        Mdot(i,j)  = delzbar*((Press(i+1,j) - Press(i-1,j)./(2*delxbar))*(-(h*C)^3/(12
    end
end

Mf = 0;
for i = 2:N-1
    for j = 2:M-1
        if Mdot(i,j) > Mf
            Mf = Mdot(i,j);
        end
    end
end

end
```

```
    (OBJECTIVE FUNCTION)

%% SCALARIZATION OF THE OBJECTIVE FUNCTION
function [Obj] = ObjFun(H)

Fric_init = 46.4385; Mf_init = 0.0215; Load = 1.0077e+3;

[pressure, LoadCap, Friction, mu, Mf] = GenProfReyEqn(H);

F_f = Friction/Fric_init;

s_w = 1/min(1, ((LoadCap/ Load)^3));


Obj= F_f * s_w;

end
```

(GENETIC ALGORITHM)

```
function [x,fval,exitflag,output,population,score] = GA(nvars,lb,ub)
%% This is an auto generated MATLAB file from Optimization Tool.
nvars = 5;
h0 = 4.6959e-04;

lb = h0 .* [0.0064  0.0064  0.0064  0.0064  0.0064];
ub = h0 .* [35  35 35 35  35];

%% Start with the default options
options = optimoptions('ga');
%% Modify options setting
options = optimoptions(options,'Display', 'off');
options = optimoptions(options,'PlotFcn', { @gaplotbestf });
[x,fval,exitflag,output,population,score] = ...
ga(@ObjFun,nvars,[],[],[],[],lb,ub,[],[],options);
```